Electronic Supplementary Material (ESI) for ChemComm.

Electronic Supplementary Information for:

Toward multifunctional anticancer therapeutics: Post-synthetic carbonate functionalization of asymmetric Au(I) bis-*N*-heterocyclic carbenes

Sajal Sen,[a] Mark W Perrin,[a] Adam C. Sedgwick,[a] Evie Y. Dunsky,[a] Vincent M. Lynch,[a] Xiao-Peng He,[b] Jonathan L. Sessler,[a*] Jonathan F. Arambula.[a*]

[a]Department of Chemistry, The University of Texas at Austin, 105 E 24th Street A5300, Austin, TX 78712-1224, United States.

[b]Key Laboratory for Advanced Materials and Joint International Research Laboratory of Precision Chemistry and Molecular Engineering, Feringa Nobel Prize Scientist Joint Research Center, School of Chemistry and Molecular Engineering, Frontiers Center for Materiobiology and Dynamic Chemistry, East China University of Science and Technology, 130 Meilong Road, Shanghai 200237, People's Republic of China.

Corresponding author e-mails: sessler@cm.utexas.edu, jfarambula@cm.utexas.edu.

Table of Contents

1. Materials and Methods

All chemical reactions were conducted under an nitrogen atmosphere using Schlenk techniques unless otherwise noted. The glassware was oven dried at 120 °C before use. All materials were obtained from commercial sources at the highest purity available and used without further purification. Chloro (dimethylsufide) gold(I) was purchased from Sigma-Aldrich. Complex **[1] [PF_6]** was synthesized according to a reported procedure.[1] **Morpho-Np-OH** was also synthesized according to a previously published protocol.[2] A modified synthesis for **2** is reported here. Solvents were either dried with a solvent purification system (dichloromethane (DCM), acetonitrile, methanol) or dried over molecular sieves (toluene) (3 Å) and degassed prior to use.

The reported ^{1}H NMR and ^{13}C NMR spectra were measured on Varian Inova spectrometers at The University of Texas at Austin using CD_2Cl_2 and DMSO-d_6 as the deuterated solvents. Chemical shifts are reported relative to the residual solvent proton signals. For the spin multiplicities the following abbreviations were used: s (singlet), d (doublet), t (triplet) and m (multiplet), as well as appropriate combinations of these. Coupling constants for protons (*J*) are given in Hertz (Hz). The NMR spectra were analyzed using the software *MestReNova v.10.0.2-15465* (Mestrelab Research S.L.). All deuterated solvents were purchased from Cambridge Isotope Laboratories. High-resolution electrospray ionization (ESI) mass spectra were recorded on a VG ZAB2E instrument or VG AutoSpec apparatus. Column chromatography was performed on Sorbent silica gel (40-63 μm). Analytical thin layer chromatography (TLC) analyses were carried on glass-backed silica gel plates (200 μm, Sorbent Technologies). Fluorescence spectroscopic measurements were made using an Agilent Cary Eclipse fluorescence spectrofluorometer. Analytical and semi-preparative RP-HPLC were performed on a Thermo Scientific Dionex Ultimate 3000 instrument equipped with a PDA detector. The analytical column was a Syncronis C18 column, 5 μm, 4.6 x 250 mm (Thermo Scientific); the mobile phase containing 0.1% acetic acid consisted of an increasing gradient from 10% acetonitrile/water to 99% acetonitrile/water over 30 min at a flow rate of 1.2 ml/min. BSA was purchased from Sigma-Aldrich and used without further purification. All fluorescence measurements for the titrations against BSA were recorded from 300 to 400 nm with an excitation wavelength of 290 nm. The emission and excitation slit widths were fixed at 5 mm. In these measurements, 20 μM BSA stock solutions were prepared in PBS buffer and diluted down to 5 μM. The approximate concentration of BSA in the resulting stock solutions was determined spectrophotometrically using a molar extinction coefficient of 43,824 M^{-1} cm^{-1} at 279 nm. For the titrations themselves, 5 mM solutions of the complex in question was used as the working solution with 1 μl aliquots being used for each addition into a 3 ml volume of the BSA stock solution. Respective blanks were subtracted from the spectra.

The fluorescence data obtained were analysed according to linear Stern-Volmer equation. [3-5]

$$\frac{F_0}{F} = K_{SV}[\mathrm{Q}] + 1 = k_q\tau_0 + 1$$

where, F_0 and F are the fluorescence intensities in the absence and presence of quenchers Q (i.e., complex **1** and complex **5** in this study), K_{SV} is the Stern–Volmer quenching constant (measuring the efficiency of quenching), k_q is the bimolecular rate constant of the quenching reaction and τ_0 is the average integral fluorescence life time of tryptophan which is ~5x10^{-9} s.[3-5] For the quenching process, the binding constant and the number of binding site were obtained from a modified Stern-Volmer equation.[3-5]

$$\log\left(\frac{F_0}{F} - 1\right) = \log k_b + n\log[\mathrm{Q}]$$

where, k_b is the binding constant, n is the number of binding sites, [Q] is the concentration of quencher i.e. complex **1** and complex **5** in this study. As noted in the literature, the nature of the quenching process (dynamic or static) can be determined from the bimolecular rate constants obtained for each complex.[3-4,6-7]

Common abbreviations used:

DCM = dichloromethane.
DEE = diethyl ether.
TEA = triethylamine.
ACN = acetonitrile.
DMAP = dimethylaminopyridine.
BSA = bovine serum albumin.

2. Synthesis

Synthesis of intermediate 2:

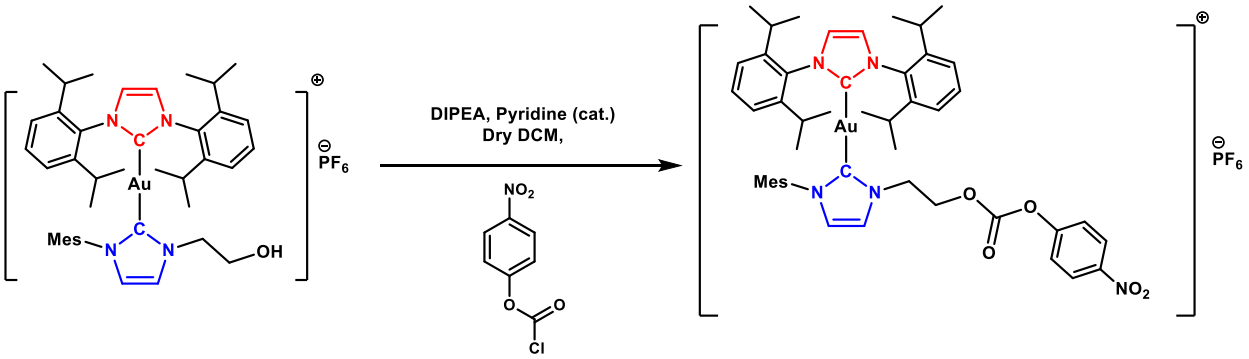

[1][PF$_6$] (300 mg, 0.312 mmol, 1 equiv.) and 4-nitrophenyl chloroformate (377.3 mg, 1.872 mmol, 6 equiv.) were combined in an oven-dried two-neck round bottom and kept under vacuum for 15 min. Dry DCM (7 ml) and dry DIPEA (75 µl, 0.468 mmol, 1.5 equiv.) were added to the mixture. Dry pyridine (30 µl) was then added to the mixture. The resulting solution was stirred for 48 h to achieve the full conversion as indicated by LCMS. The volatiles were evaporated off and diethyl ether was added. A white solid precipitated out after stirring for 15 mins and subjecting to trituration. The solid obtained in this way was collected via filtration and washed several times with diethyl ether. The solid was placed in a 20 ml scintillation vial and 5 ml of nanopore water was added. The reaction mixture was then stirred for 15 min. Finally, the resulting white suspension was collected by filtration, washed with 5 ml water and diethyl ether, and left to dry under air. All characterization results matched with those previously reported.[1] **Yield:** 306 mg (87%).

General synthesis of carbonates via protocol 1:

Precursor **2** (1 equiv.) was kept under vacuum for 15 mins in an oven-dried two-neck round bottomed flask. Dry DCM (4 ml) and the aromatic alcohol of interest (3 equiv.) were then added. After stirring the mixture for 10 min, dry TEA (2 equiv.) was added and whole mixture was stirred under an N_2 atmosphere for 24 h. After confirming the completion of the reaction by LCMS, the volatiles were evaporated off and diethyl ether was added. The solid precipitate that resulted was collected by filtration. The solid was repeatedly washed with diethyl ether and dried under air.

Synthesis of 4:

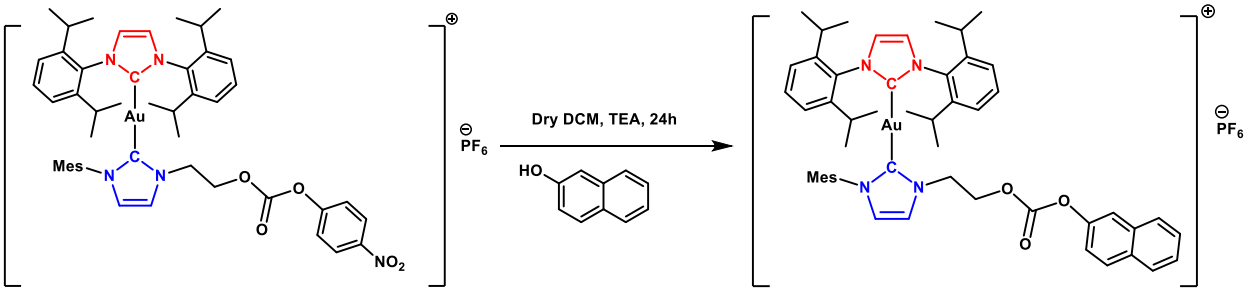

Precursor **2** (40 mg, 0.035 mmol) was used along with β-naphthol (15 mg, 0.105 mmol, 3 equiv.) and dry TEA (10 µl, 0.070 mmol, 2 equiv.) with the reaction run in 5 ml dry DCM. A white microcrystalline powder was obtained as the product. Crystals were grown via slow diffusion using DCM/diethyl ether. **Yield:** 29 mg (74%). **ESI-HRMS (acetonitrile) (m/z):** Calculated for $[C_{52}H_{60}N_4O_3Au]^+$: 985.4326. Found: 985.4340.

^{1}H NMR (500 MHz, DMSO-*d*$_6$) δ 8.07 (s, 2H), 7.99 (t, *J* = 7.9 Hz, 2H), 7.95 – 7.91 (m, 1H), 7.74 (d, *J* = 1.9 Hz, 1H), 7.65 (d, *J* = 2.5 Hz, 1H), 7.63 – 7.53 (m, 4H), 7.41 (d, *J* = 1.8 Hz, 1H), 7.34 (d, *J* = 7.8 Hz, 4H), 7.27 (dd, *J* = 8.9, 2.5 Hz, 1H), 6.76 (s, 2H), 4.10 (t, *J* = 5.0 Hz, 2H), 3.97 (t, *J* = 5.0 Hz, 2H), 2.43 – 2.30 (m, 7H), 1.55 (s, 6H), 1.16 (d, *J* = 6.8 Hz, 12H), 1.09 (d, *J* = 6.9 Hz, 12H).

^{13}C{^{1}H} NMR (126 MHz, DMSO-*d*$_6$) δ 186.2, 182.9, 153.1, 148.5, 145.5, 138.9, 134.4, 134.1, 133.9, 133.6, 131.6, 130.9, 130.1, 129.5, 128.2, 128.0, 127.4, 126.6, 125.5, 124.2, 123.7, 121.0, 118.3, 67.0, 49.3, 28.7, 24.2, 24.1, 21.2, 17.1.

Synthesis of 8:

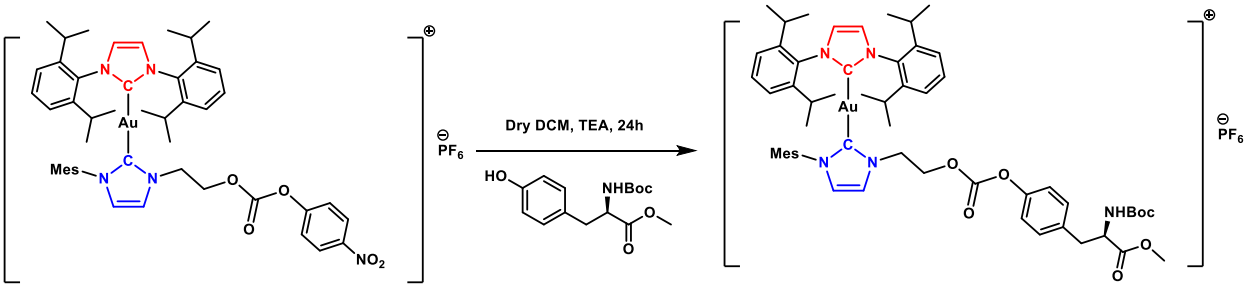

Precursor **2** (40 mg, 0.035 mmol) was used along with methyl (*tert*-butoxycarbonyl)-L-tyrosinate (31 mg, 0.105 mmol, 3 equiv.) and dry TEA (10 µl, 0.070 mmol, 2 equiv.) with the reaction run in 5 ml dry DCM. The product was obtained as a white microcrystalline powder. **Yield:** 27 mg (60%). **ESI-HRMS (acetonitrile) (m/z):** Calculated for $[C_{57}H_{73}N_5O_7Au]^+$: 1136.5176. Found: 1136.5160.

^{1}H NMR (500 MHz, DMSO-*d*$_6$) δ 8.07 (s, 2H), 7.68 (d, *J* = 2.0 Hz, 1H), 7.60 (t, *J* = 7.8 Hz, 2H), 7.37 (d, *J* = 1.8 Hz, 1H), 7.33 (d, *J* = 7.8 Hz, 5H), 7.27 (d, *J* = 8.1 Hz, 2H), 7.01 (d, *J* = 8.2 Hz, 2H), 6.75 (s, 2H), 4.18 (td, *J* = 9.7, 8.5, 5.1 Hz, 1H), 4.05 (t, *J* = 5.1 Hz, 2H), 3.93 (t, *J* = 5.1 Hz, 2H), 3.62 (s, 3H), 3.01 (dd, *J* = 13.9, 5.0 Hz, 1H), 2.85 (dd, *J* = 13.8, 10.3 Hz, 1H), 2.35 (q, *J* = 7.1 Hz, 7H), 1.54 (d, *J* = 2.6 Hz, 6H), 1.32 (s, 9H), 1.16 (d, *J* = 6.9 Hz, 12H), 1.08 (d, *J* = 6.9 Hz, 12H).

$^{13}C\{^{1}H\}$ NMR (126 MHz, DMSO-d_6) δ 186.1, 182.8, 172.9, 155.9, 153.0, 149.6, 145.5, 138.9, 136.2, 134.1, 133.9, 130.9, 130.7, 129.5, 125.5, 124.3, 124.1, 123.6, 121.1, 78.8, 66.8, 55.5, 52.3, 49.2, 46.2, 36.2, 28.7, 28.6, 24.3, 24.1, 21.3, 17.1.

General synthesis of carbonates via protocol 2:

Precursor **2** (1 equiv.) and dry DMAP (3 equiv.) were kept under vacuum for 5 mins in an oven-dried two-neck round bottomed flask. Dry DCM (4 ml) and the alcohol of interest (3 equiv.) were then added. The whole mixture was stirred under N_2 atmosphere for 24 h. After confirming the completion of the reaction by LCMS, the volatiles were evaporated off. Diethyl ether was then added to the residue. The solid precipitate that resulted was collected by filtration, washed with diethyl ether, and dried under air. Finally, it was purified by means of a small silica gel chromatography column using 5% MeOH/95% DCM collecting the fraction at R_f ~ 0.4. (NB: DMAP sticks to the column). The appropriate fractions were collected and concentrated under reduced pressure before hexanes were added to produce a white precipitate. The solid was collected by filtration and washed with hexanes several times to give the final product as a white fluffy powder.

Synthesis of 5:

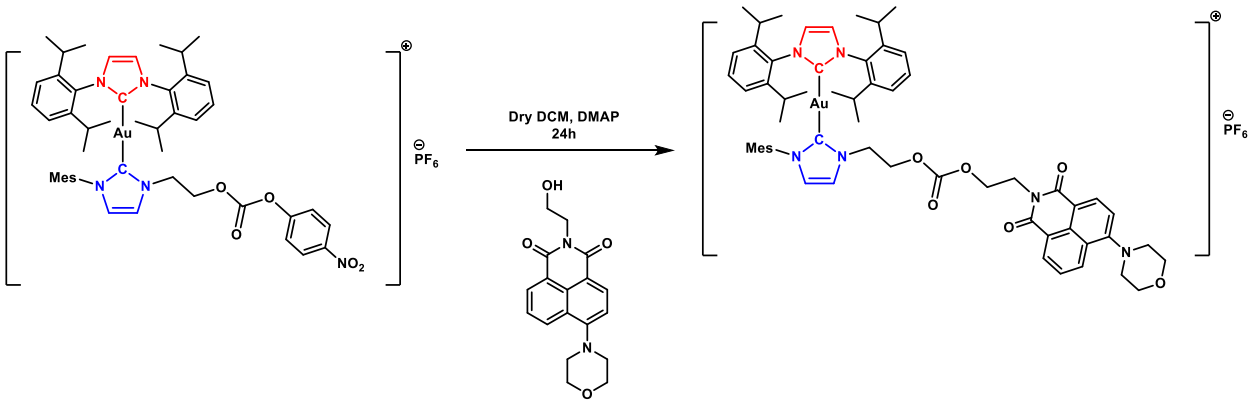

Precursor **2** (40 mg, 0.035mmol) was used along with **Morpho-Np-OH** (20 mg, 0.056 mmol, 1.6 equiv.) and dry DMAP (13 mg, 0.105 mmol, 3 equiv.) with the reaction run in 5 ml dry DCM. The product was obtained as a yellow microcrystalline powder. Crystals could be grown from DCM/diethyl ether via slow diffusion. **Yield:** 19 mg (40%). **ESI-HRMS (acetonitrile) (m/z):** Calculated for $[C_{60}H_{70}N_6O_6Au]^+$: 1167.5017. Found: 1167.5015.

^{1}H NMR (500 MHz, DMSO-d_6) δ 8.53 (t, *J* = 7.1 Hz, 2H), 8.45 (d, *J* = 8.1 Hz, 1H), 8.02 (s, 2H), 7.86 (t, *J* = 7.9 Hz, 1H), 7.59 (d, *J* = 1.9 Hz, 1H), 7.51 (t, *J* = 7.8 Hz, 2H), 7.40 (d, *J* = 8.2 Hz, 1H), 7.26 – 7.18 (m, 5H), 6.72 (s, 2H), 4.32 (s, 4H), 3.92 (t, *J* = 4.4 Hz, 4H), 3.88 (t, *J* = 5.1 Hz, 2H), 3.80 (t, *J* = 5.2 Hz, 2H), 3.22 (t, *J* = 4.5 Hz, 4H), 2.35 (s, 3H), 2.27 (h, *J* = 7.0 Hz, 4H), 1.48 (s, 6H), 1.08 (d, *J* = 6.9 Hz, 12H), 0.98 (d, *J* = 6.9 Hz, 12H).

$^{13}C\{^{1}H\}$ NMR (126 MHz, DMSO-d_6) δ 186.1, 182.7, 164.2, 163.7, 156.1, 154.4, 145.4, 138.8, 134.3, 134.0, 133.8, 132.9, 131.3, 130.8, 129.8, 129.4, 126.7, 125.8, 125.4, 124.2, 123.8, 123.4, 122.9, 116.2, 115.6, 66.6, 66.1, 65.4, 53.5, 49.2, 38.8, 28.6, 24.1, 24.0, 21.2, 17.0.

Synthesis of 6:

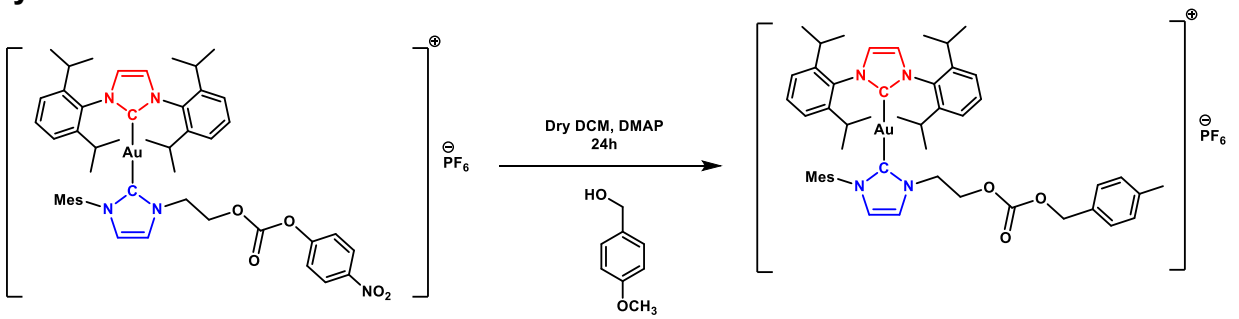

Precursor **2** (40 mg, 0.035 mmol) was used along with *p*-tolylmethanol (13 mg, 0.105 mmol, 3 equiv.) and dry DMAP (13 mg, 0.105 mmol, 3 equiv.) with the reaction run in 5 ml dry DCM. The product was obtained as a white microcrystalline powder. Crystals could be grown via slow diffusion using DCM/diethyl ether. **Yield:** 21 mg (54%). **ESI-HRMS (acetonitrile) (m/z):** Calculated for $[C_{50}H_{62}N_4O_3Au]^+$: 963.4487. Found: 963.4467.

^{1}H NMR (400 MHz, DMSO-*d*$_6$) δ 8.02 (s, 2H), 7.57 (d, *J* = 1.9 Hz, 1H), 7.52 (t, *J* = 7.8 Hz, 2H), 7.29 – 7.21 (m, 5H), 7.21 – 7.14 (m, 4H), 6.72 (s, 2H), 4.97 (s, 2H), 3.90 (t, *J* = 5.2 Hz, 2H), 3.82 (t, *J* = 5.5 Hz, 2H), 2.35 – 2.24 (m, 10H), 1.50 (s, 6H), 1.11 (d, *J* = 6.8 Hz, 12H), 1.01 (d, *J* = 6.9 Hz, 12H).

^{13}C{^{1}H} NMR (126 MHz, DMSO-*d*$_6$) δ 186.1, 182.8, 172.9, 155.9, 153.0, 149.6, 145.5, 138.9, 136.2, 134.1, 133.9, 130.9, 130.7, 129.5, 125.5, 124.3, 124.1, 123.6, 121.1, 78.8, 66.8, 55.5, 52.3, 49.2, 46.2, 36.2, 28.7, 28.6, 24.3, 24.1, 21.3, 17.1.

Synthesis of 7:

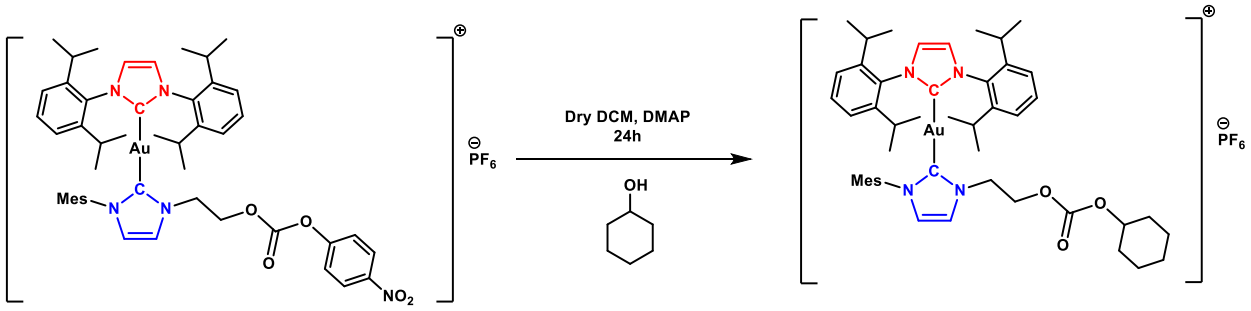

Precursor **2** (40 mg, 0.035mmol) was used along with cyclohexanol (11 µl, 0.105 mmol, 3 equiv.) and dry DMAP (13 mg, 0.105 mmol, 3 equiv.) in 5 ml dry DCM. The product was obtained as a white microcrystalline powder. Crystals could be grown via slow diffusion using DCM/diethyl ether. However, the resulting crystals proved hard to mount and did not diffract well. **Yield:** 15 mg (43%). **ESI-HRMS (acetonitrile) (m/z):** Calculated for $[C_{48}H_{64}N_4O_3Au]^+$: 941.4644. Found: 941.4638.

^{1}H NMR (400 MHz, DMSO-*d*$_6$) δ 8.03 (s, 2H), 7.59 – 7.51 (m, 3H), 7.32 – 7.25 (m, 5H), 6.72 (s, 2H), 4.37 (s, 1H), 3.88 (d, *J* = 5.1 Hz, 2H), 3.80 (d, *J* = 5.3 Hz, 2H), 2.31 (d, *J* = 8.2 Hz, 7H), 1.69 (s, 2H), 1.58 (s, 2H), 1.52 (s, 6H), 1.42 (s, 1H), 1.27 (q, *J* = 9.4 Hz, 5H), 1.12 (d, *J* = 6.8 Hz, 12H), 1.04 (d, *J* = 6.8 Hz, 12H).

$^{13}C\{^{1}H\}$ NMR (126 MHz, DMSO-d_6) δ 186.2, 182.8, 153.9, 145.5, 138.9, 134.4, 134.1, 133.9, 130.9, 129.5, 125.5, 124.3, 123.9, 123.4, 76.6, 65.6, 49.2, 31.3, 28.7, 25.1, 24.3, 24.1, 23.3, 21.3, 17.1.

Synthesis of 9:

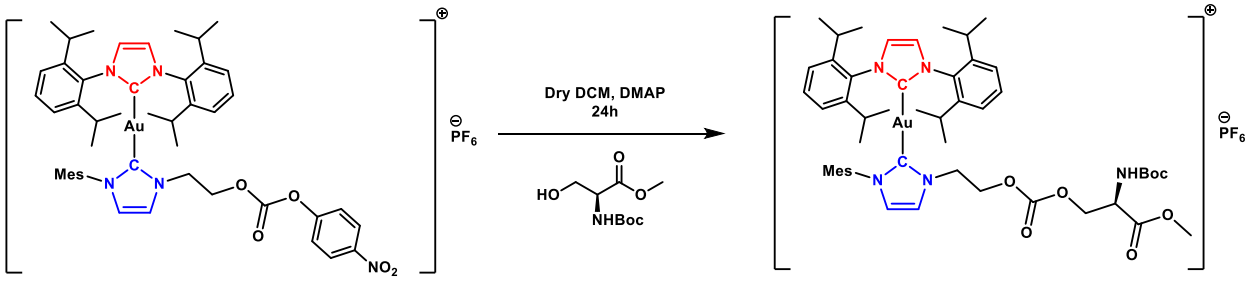

Precursor **2** (40 mg, 0.035 mmol) was used along with methyl (*tert*-butoxycarbonyl)-L-serinate (commercially available as 95% pure) (22 µl, 0.105 mmol, 3 equiv.) and dry DMAP (13 mg, 0.105 mmol, 3 equiv.) in 5 ml dry DCM. White microcrystalline powder was obtained as product. **Yield:** 18 mg (43%). **ESI-HRMS (acetonitrile) (m/z):** Calculated for $[C_{51}H_{69}N_5O_7Au]^+$: 1060.4857. Found: 1060.4874.

^{1}H NMR (400 MHz, DMSO-d_6) δ 8.02 (s, 2H), 7.59 – 7.51 (m, 3H), 7.35 (d, *J* = 7.6 Hz, 1H), 7.32 – 7.24 (m, 5H), 6.72 (s, 2H), 4.25 (d, *J* = 9.2 Hz, 2H), 4.11 (d, *J* = 10.0 Hz, 1H), 3.96 – 3.76 (m, 4H), 3.61 (s, 3H), 2.31 (q, *J* = 6.9, 5.6 Hz, 7H), 1.52 (s, 6H), 1.34 (s, 9H), 1.12 (d, *J* = 6.9 Hz, 12H), 1.04 (d, *J* = 6.8 Hz, 12H).

$^{13}C\{^{1}H\}$ NMR (126 MHz, DMSO-d_6) δ 186.1, 182.7, 170.3, 155.8, 154.1, 145.5, 138.9, 134.3, 133.9, 130.9, 129.5, 125.5, 124.3, 123.9, 123.6, 79.1, 66.7, 66.4, 52.9, 52.7, 49.1, 31.4, 28.7, 28.6, 24.3, 24.1, 22.5, 21.3, 17.1, 14.4.

Synthesis of 10:

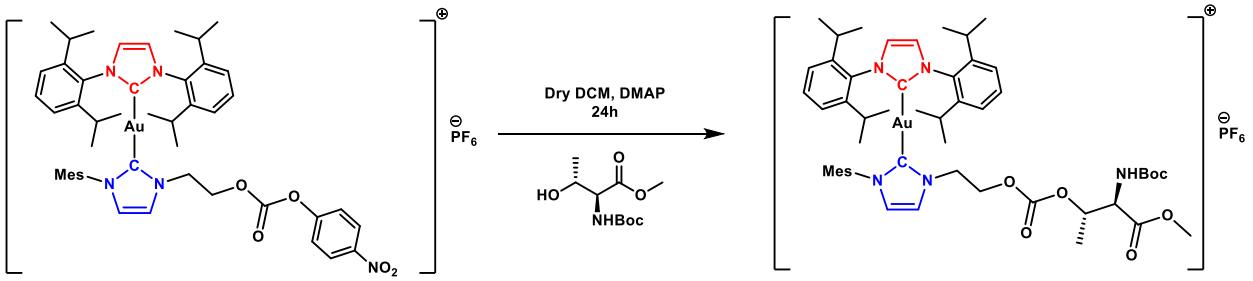

Precursor **4** (40 mg, 0.035 mmol) was used along with methyl (*tert*-butoxycarbonyl)-L-threoninate (commercially available in 95% purity) (22 µl, 0.105 mmol, 3 equiv.) and dry DMAP (13 mg, 0.105 mmol, 3 equiv.) with the reaction run in 5 ml dry DCM. The product was obtained as a white microcrystalline powder. **Yield:** 14 mg (33%). **ESI-HRMS (acetonitrile) (m/z):** Calculated for $[C_{52}H_{71}N_5O_7Au]^+$: 1074.5014. Found: 1074.5013.

^{1}H NMR (500 MHz, DMSO-d_6) δ 8.06 (d, *J* = 10.4 Hz, 2H), 7.60 (t, *J* = 7.8 Hz, 2H), 7.56 (d, *J* = 1.9 Hz, 1H), 7.33 (d, *J* = 8.0 Hz, 5H), 7.15 (d, *J* = 8.6 Hz, 1H), 6.76 (s, 2H), 4.91 (q, *J* = 5.4 Hz, 1H), 4.30 (dd, *J* = 8.7,

4.3 Hz, 1H), 4.04 – 3.72 (m, 4H), 3.63 (s, 3H), 2.36 (q, *J* = 6.4, 5.7 Hz, 7H), 1.62 – 1.51 (m, 6H), 1.40 (s, 9H), 1.17 (d, *J* = 6.6 Hz, 15H), 1.08 (dt, *J* = 6.4, 3.1 Hz, 12H).

$^{13}C\{^{1}H\}$ NMR (126 MHz, DMSO-d_6) δ 186.1, 182.7, 170.5, 156.0, 153.5, 145.5, 138.9, 134.1, 133.9, 130.9, 129.5, 125.5, 124.3, 123.9, 123.6, 79.2, 74.2, 66.3, 57.2, 52.7, 49.2, 34.7, 31.4, 28.7, 28.6, 24.3, 24.1, 22.5, 21.3, 17.1, 16.7, 14.4.

Types of alcohol	Example	Protocol	Yield[a](%)
Aromatic	**4**	**1**	**74**
Primary	**5**	**2**	**40**
Benzylic	**6**	**2**	**54**
Secondary	**7**	**2**	**43**
Modified tyrosine	**8**	**1**	**60**
Modified serine	**9**	**2**	**43**
Modified threonine	**10**	**2**	**33**

Table S1: Types of alcohols attached via present methodology. ([a] Yields were calculated based on isolated product).

3. HPLC Experimental Results

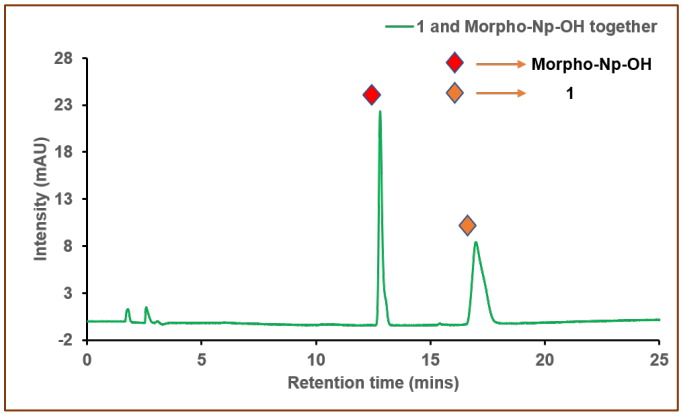

Fig. S1: HPLC trace of complex **1** and **Morpho-Np-OH**. The retention time for **Morpho-Np-OH** is 12.5 min whereas complex **1** elutes at around 17.3 min.

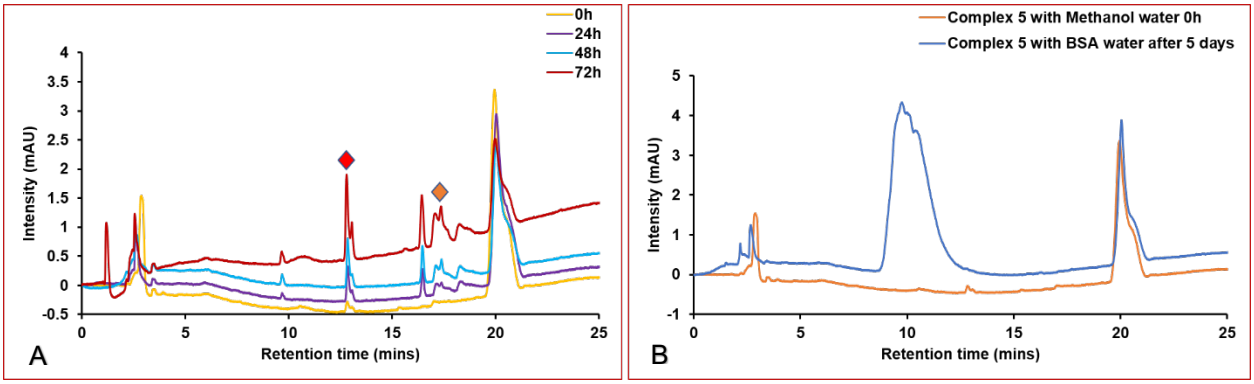

Fig. S2: HPLC diagram showing: (A) Gradual degradation of a 2% DMSO solution of complex **5** (100 μM) into complex **1** and **Morpho-Np-OH** in the presence of 98% 1:1 methanol/PBS upon incubation at 37° C. Methanol was used to ensure complete dissolution of complex **5** during this 96 h study. (B) 2% DMSO solution of complex **5** (100 μM) in 98% PBS in the presence of 600 μM BSA. No evidence of degradation was seen even after 6 days upon incubating at 37° C.

4. Fluorescence Experiments and Tests of Solubility

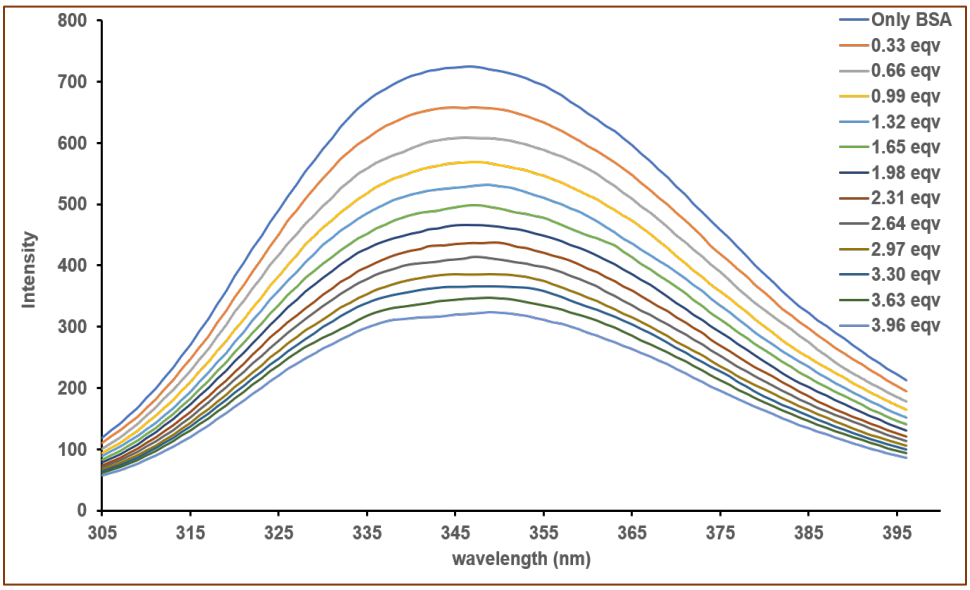

Fig. S3: Fluorescence intensity quenching of BSA (5 μM) seen in the presence of increasing equivalents of **5**. Excitation wavelength used: 290 nm. Excitation slit width: 5 mm, emission slit width: 5 mm.

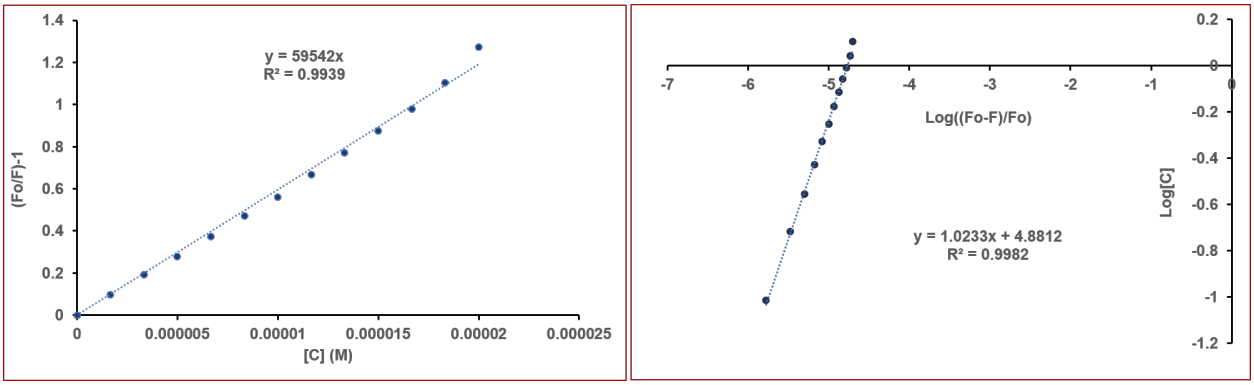

Fig. S4: Stern-Volmer plot and double logarithm plot for the fluorescence quenching of BSA observed upon treatment with complex **5**.

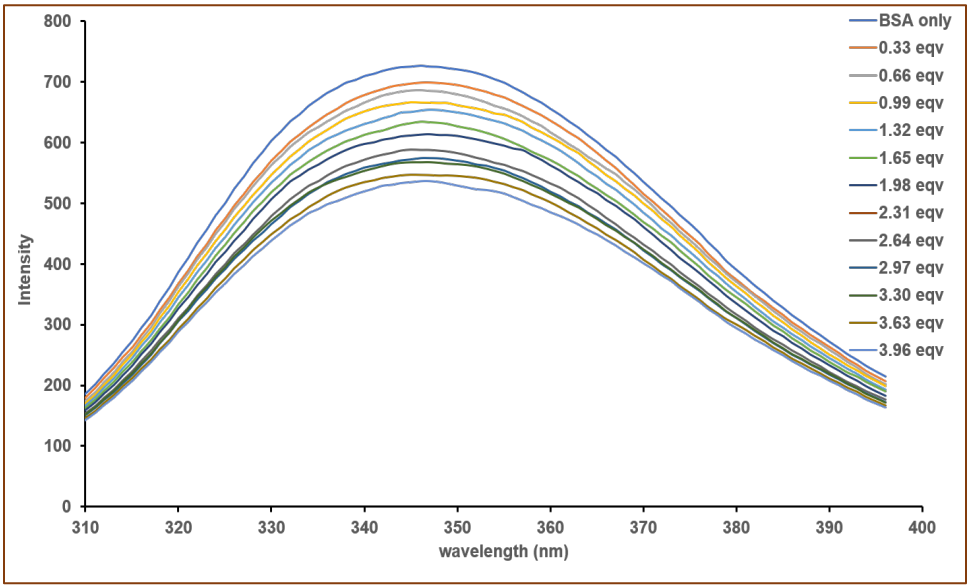

Fig. S5: Quenching of the fluorescence intensity of BSA (5 μM) seen upon treating with increasing equivalents of **1**. Excitation wavelength used: 290 nm. Excitation slit width: 5 mm, emission slit width: 5 mm.

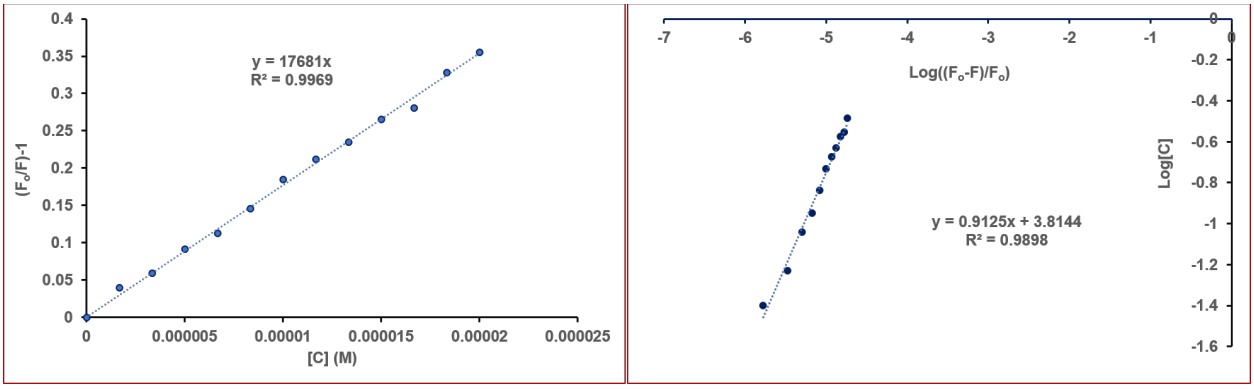

Fig. S6: Stern-Volmer plot and double logarithm plot for the fluorescence quenching of BSA observed in the presence of complex **1**.

Compound	K_{SV} (M^{-1})	K_q (M^{-1} s^{-1})	K_b (M^{-1})	n
1	$1.76*10^4$	$3.54*10^{12}$	$6.45*10^3$	~1 (0.912)
5	$5.95*10^4$	$1.19*10^{13}$	$7.58*10^4$	~ 1 (1.023)

Table S2: Stern–Volmer data for the studies of the Au NHC complexes **1** and **5** with albumin, as calculated from the fluorescence quenching experiments. The binding constant (K_b) and the number of binding sites (n) for each metal complex with albumin, as calculated from double-logarithm plots, are included in this table.

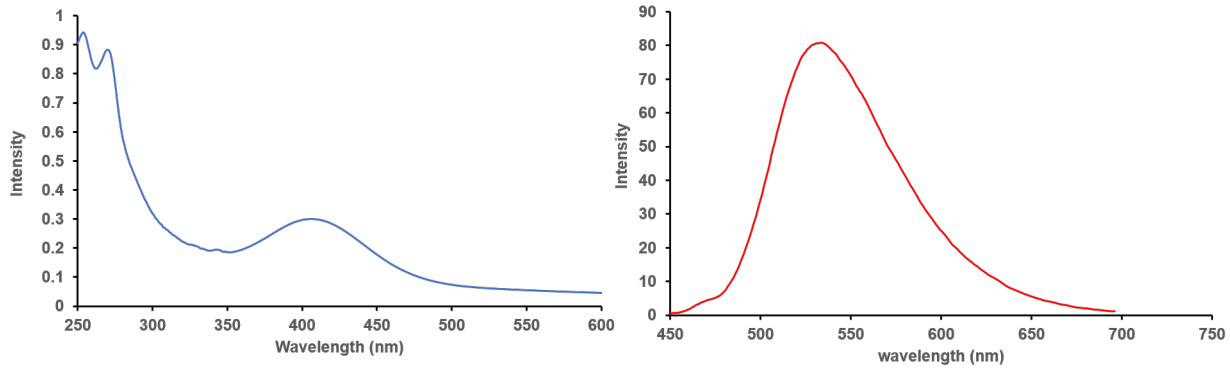

Fig. S7: (Left) UV absorption spectrum of a 10 μM solution of complex **5** in 2% DMSO/PBS. (Right) Fluorescence spectrum of a 1 μM solution of complex **5** in 0.2% DMSO/PBS. Excitation wavelength: 405 nm, excitation slit width: 5 mm, emission slit width: 10 mm.

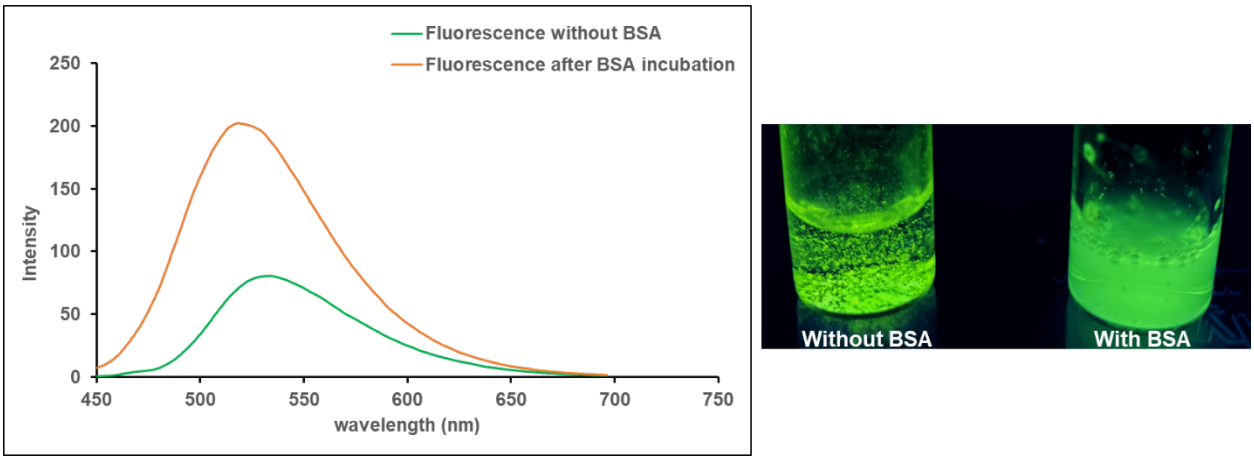

Fig. S8: (Left) Fluorescence spectrum of complex **5** (1 μM) recorded in the absence and presence of 20 μM BSA in PBS. (Right) Complex **5** (100 μM) precipitates out as aggregates in the absence of BSA in PBS, whereas in the presence of 600 μM BSA **5** is solubilized.

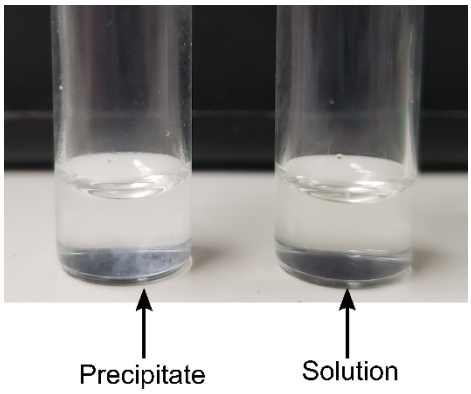

Fig. S9: 2% DMSO solutions of **1** (100 μM) photographed in the absence (left) and after adding BSA and letting sit 15 min (right).

5. Biological Experiments

Cell proliferation studies: A549 cells were harvested and seeded into 96-well culture plates (Costar 07-200-90) in 100 μL of culture medium. The cells were allowed to incubate overnight at 37 ºC in the presence of 5% CO_2. A549 cells were seeded at a density of 1500 cells/well. The next day, appropriate serial dilutions of drug stocks in culture media were made. To each well of a 96 well plate was added 100 μL of the appropriate solution. After a total of three days, a 50 mL aliquot of 3 mg/mL tetrazolium dye, 3-(4,5-dimethylthiazol-2-yl)-2,5-diphenyltetrazolium bromide (Alfa Aesar L11939), dissolved in culture medium without fetal bovine serum (FBS), was added to each well, followed by a 4 h incubation period at 37 ºC. After removal of the medium, the resulting formazan was dissolved in 50 mL DMSO and the respective absorbances were measured at 560–650 nm using a microplate reader (Molecular Devices, Sunnyvale, CA). Absorbance values were corrected for background and then normalized to wells containing untreated cells to allow for plate-to-plate comparisons. The resulting dose response curves were subjected to linear regression analysis (Origin by OriginLab, Inc.) for determination of IC_{50} values. The data are shown as mean inhibition of proliferation or growth as a percentage of control cells and are from 3 replicate experiments. Maximum concentration of DMSO used is 0.1%. This concentration of DMSO was determined to be non-toxic in separate control experiments. To evaluate the cytotoxicity of BSA-treated **5**, 100 μM of complex **5** was incubated with 40 mg/ml (600 μM) BSA at 37° C for 1 h (final DMSO conc. 2%). The stock solution was further diluted 10-fold in RPMI media such that the maximum drug concentration used was 10 μM for the dose dependent MTT assay.

Confocal Fluorescence microscopy: Tumor cells were harvested and seeded at a density of 2 x 10^5 cells/dish in 35 mm dishes containing a poly-D lysine coated 10 mm glass diameter (Mat Tek P35GC-1.5-10-C) overnight. Cells were then incubated with respective doses of different complexes at 37 ºC for 4 h. Post incubation, the media was removed and cells were washed (2x) with PBS. To the cells was added a PBS solution containing 50 nM Mitotracker® Red FM (Lifetech M22425) for 30 min at 37 ºC. After incubation, the dye PBS solution was removed and the cells were washed with PBS (2x). The cells were then imaged fluorescently on a Zeiss LSM 710 laser scanning confocal microscope using a Plan-Apo 63x/1.4 oil objective. The green channel was excited with a 405 nm laser, and the emission was detected spectrally from 482 - 555 nm. The red channel was excited with a 561 nm laser, and the emission was detected spectrally from 573 - 639 nm. For the BSA pretreated studies, a 100 μM solution of complex **5** was incubated with 40 mg/ml (600 μM) BSA at 37° C for 1 h (final DMSO conc. 2%). The stock solution was further diluted 100-fold in RPMI media giving **5** at a final concentration of 1 μM.

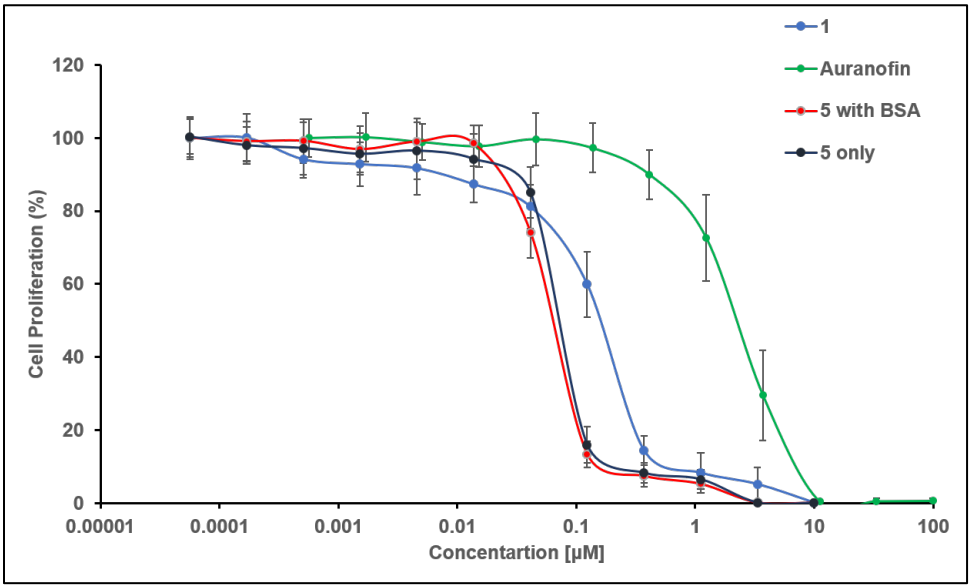

Fig. S10: Cell proliferation profiles of A549 lung cancer cells treated with complex **1** and complex **5** in the presence and absence of BSA, respectively (72 h drug incubation time). Auranofin was used as a reference drug (maximum DMSO: 0.1%).

6. Crystallographic Analyses

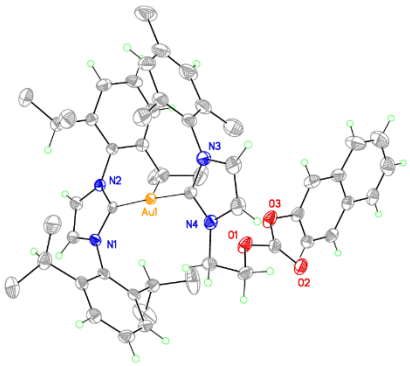

Fig. S11: View of the complex in **4** showing the heteroatom labeling scheme. Displacement ellipsoids are scaled to the 50% probability level. The methyl group hydrogen atoms were omitted for clarity.

X-ray experimental for **4** ($C_{21}H_{36}N_2$) Au($C_{31}H_{24}N_2O_3$)PF_6: Crystals grew as clusters of colorless plates by slow evaporation of diethyl ether in dichloromethane solution. The data crystal was separated from a cluster of crystals and had approximate dimensions; 0.25 x 0.19 x 0.067 mm. The data were collected on an Agilent Technologies SuperNova Dual Source diffractometer using a μ-focus Cu Kα radiation source (λ = 1.5418 Å) with collimating mirror monochromators. A total of 889 frames of data were collected using ω-scans with a scan range of 1° and a counting time of 6 seconds per frame for frames collected with a detector offset of +/- 41.7° and 20 seconds per frame with frames collected with a detector offset of 107.1°. The data were collected at 100 K using an Oxford Cryostream low temperature device. Details of the crystal data, data collection and structure refinement are listed in Table S3. Data collection, unit cell refinement and data reduction were performed using Rigaku Oxford Diffraction's CrysAlisPro V 1.171.40.53.[8] The structure was solved by direct methods using SHELXT[9] and refined by full-matrix least-squares on F^2 with anisotropic displacement parameters for the non-H atoms using SHELXL-2016/6.[10] Structure analysis was aided by use of the programs PLATON,[11] OLEX2[12] and WinGX.[13] The hydrogen atoms on the carbon atoms were calculated in ideal positions with isotropic displacement parameters set to 1.2xU_{eq} of the attached atom (1.5xU_{eq} for methyl hydrogen atoms).

The function, $\Sigma w(|Fo|^2 - |Fc|^2)^2$, was minimized, where $w = 1/[(\sigma(F_o))^2 + (0.0543*P)^2 + (8.4243*P)]$ and $P = (|F_o|^2 + 2|F_c|^2)/3$. $R_w(F^2)$ refined to 0.0836, with R(F) equal to 0.0298 and a goodness of fit, S = 1.03. Definitions used for calculating R(F), $R_w(F^2)$ and the goodness of fit, S, are given below.[14] The data were checked for secondary extinction effects, but no correction was necessary. Neutral atom scattering factors and values used to calculate the linear absorption coefficient are from the International Tables for X-ray Crystallography (1992).[15] All figures were generated using SHELXTL/PC.[16]

Table S3. X-ray structural details for **4** ($C_{21}H_{36}N_2$) Au($C_{31}H_{24}N_2O_3$)PF_6

CCDC number	1999229
Empirical formula	C_{52} H_{60} Au F_6 N_4 O_3 P
Formula weight	1130.97
Temperature	99.9(2) K

Wavelength	1.54184 Å	
Crystal system	orthorhombic	
Space group	P b c a	
Unit cell dimensions	a = 16.47860(10) Å	α = 90°.
	b = 22.15860(10) Å	β = 90°.
	c = 27.4653(2) Å	γ = 90°.
Volume	10028.75(11) $Å^3$	
Z	8	
Density (calculated)	1.498 Mg/m^3	
Absorption coefficient	6.389 mm^{1}	
F (000)	4576	
Crystal size	0.25 x 0.19 x 0.067 mm^3	
Theta range for data collection	3.218 to 73.427°.	
Index ranges	-20<=h<=20, -27<=k<=27, -34<=l<=27	
Reflections collected	49954	
Independent reflections	9911 [R(int) = 0.0395]	
Completeness to theta = 67.684°	99.9 %	
Absorption correction	Gaussian and multi-scan	
Max. and min. transmission	1.00000 and 0.54722	
Refinement method	Full-matrix least-squares on F^2	
Data / restraints / parameters	9911 / 402 / 615	
Goodness-of-fit on F^2	1.047	
Final R indices [I>2sigma(I)]	R1 = 0.0298, wR2 = 0.0806	
R indices (all data)	R1 = 0.0320, wR2 = 0.0836	
Extinction coefficient	n/a	
Largest diff. peak and hole	1.570 and -0.974 $e.Å^{-3}$	

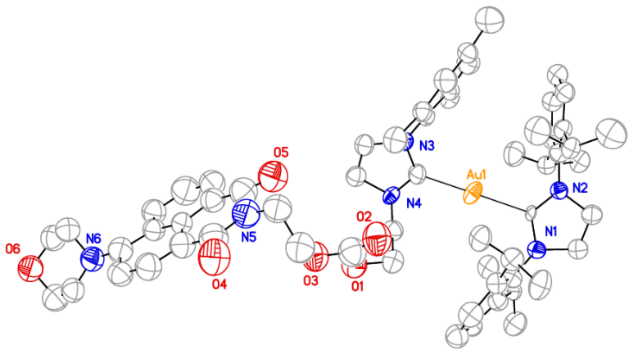

Fig. S12: View of the complex in **5** showing the heteroatom labeling scheme. Displacement ellipsoids are scaled to the 30% probability level. The hydrogen atoms were omitted for clarity.

X-ray experimental for **5** $(C_{33}H_{34}N_4O_6)Au(C_{27}H_{36}N_4)$ PF_6: Crystals grew as large, colorless prisms by slow

diffusion of DEE in chloroform. The data crystal had approximate dimensions; 0.1 x 0.01 x 0.01 mm. The data were collected on the Advanced Light Source Beamline 5.0.1 at a wavelength of 0.97741 Å. A total of 240 frames of data were collected using φ-scans with a scan range of 0.5° and a counting time of 2 second per frame. The data were collected at 100 K using an Oxford Cryostream low temperature device. Details of crystal data, data collection and structure refinement are listed in Table S4. Data collection, unit cell refinement and data reduction were performed using Agilent Technologies CrysAlisPro V 1.171.40.71a.[8] The structure was solved by direct methods using SHELXT[9] and refined by full-matrix least-squares on F^2 with anisotropic displacement parameters for the non-H atoms using SHELXL-2014/7.[10] Structure analysis was aided by use of the programs PLATON[11] and WinGX.[13] The hydrogen atoms were calculated in ideal positions with isotropic displacement parameters set to 1.2xUeq of the attached atom (1.5xUeq for methyl hydrogen atoms).

The function, $\Sigma w(|Fo|^2 - |Fc|^2)^2$, was minimized, where $w = 1/[(\sigma(F_o))^2 + (0.0543*P)^2 + (8.4243*P)]$. $R_w(F^2)$ refined to 0.338, with R(F) equal to 0.130 and a goodness of fit, S, = 2.15. Definitions used for calculating R(F), $R_w(F^2)$ and the goodness of fit, S, are given below.[14] The data were checked for secondary extinction effects but no correction was necessary. Neutral atom scattering factors and values used to calculate the linear absorption coefficient are from the International Tables for X-ray Crystallography (1992).[15] All figures were generated using SHELXTL/PC.[16]

Table S4. X-ray structural details for **5** $(C_{33}H_{34}N_4O_6)Au(C_{27}H_{36}N_4)\ PF_6$

CCDC Number	1999228	
Empirical formula	C60 H70 Au F6 N6 O6 P	
Formula weight	1313.15	
Temperature	100 K	
Wavelength	0.97741 Å	
Crystal system	triclinic	
Space group	P -1	
Unit cell dimensions	a = 10.8241(6) Å	α = 102.209(4)°.
	b = 18.2147(9) Å	β = 97.728(4)°.
	c = 32.3647(17) Å	γ = 104.498(5)°.
Volume	5918.4(6) $Å^3$	
Z	4	
Density (calculated)	1.474 Mg/m^3	
Absorption coefficient	3.797 mm^{-1}	
F(000)	2672	
Crystal size	0.1 x 0.01 x 0.01 mm^3	
Theta range for data collection	2.067 to 26.257°.	
Index ranges	-9<=h<=9, -15<=k<=14, -20<=l<=27	
Reflections collected	6065	
Independent reflections	4661 [R(int) = 0.0389]	
Completeness to theta = 26.257°	50.7 %	
Absorption correction	Semi-empirical from equivalents	
Max. and min. transmission	1.00 and 0.02	
Refinement method	Full-matrix least-squares on F^2	
Data / restraints / parameters	4661 / 1264 / 1484	
Goodness-of-fit on F2	1.718	
Final R indices [I>2sigma(I)]	R1 = 0.1301, wR2 = 0.3272	
R indices (all data)	R1 = 0.1414, wR2 = 0.3380	

Extinction coefficient	n/a
Largest diff. peak and hole	2.224 and -2.429 e.Å^{-3}

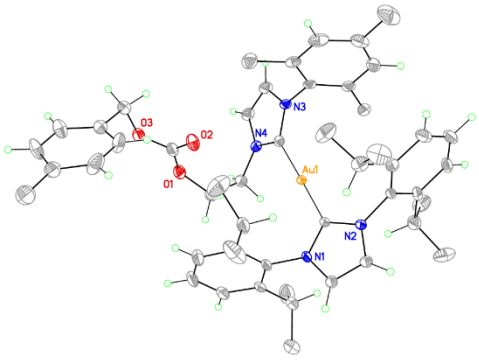

Fig. S13: View of the complex in **6** showing the heteroatom labeling scheme. Displacement ellipsoids are scaled to the 50% probability level. The methyl group hydrogen atoms were omitted for clarity.

X-ray experimental for **6** ($C_{27}H_{36}N_2$) Au($C_{23}H_{26}N_2O_3$) – PF_6: Crystals grew as clear, colorless prisms by slow evaporation from diethyl ether in dichloromethane. The data crystal was cut from a larger crystal and had approximate dimensions; 0.36 x 0.30 x 0.09 mm. The data were collected at -173°C on a Nonius Kappa CCD diffractometer using a Bruker AXS Apex II detector and a graphite monochromator with MoK_α radiation (λ = 0.71073 Å).Reduced temperatures were maintained by use of an Oxford Cryosystems 700 low-temperature device. A total of 1454 frames of data were collected using ω-scans with a scan range of 0.6° and a counting time of 27 seconds per frame. Details of crystal data, data collection and structure refinement are listed in Table S5. Data reduction were performed using SAINT V8.27B.[17] The structure was solved by direct methods using SHELXT[9] and refined by full-matrix least-squares on F^2 with anisotropic displacement parameters for the non-H atoms using SHELXL-2016/6.[10] Structure analysis was aided by use of the programs PLATON,[11] OLEX2[12] and WinGX.[13] The hydrogen atoms bound to carbon atoms were calculated in idealized positions. There is some disorder in the phenyl group bound to the carbonate portion of one of the ligands. In addition, one of the isopropyl groups was also disordered. The disorder was modeled in OLEX2 using the Split-Same function.

The function, $\Sigma w(|F_o|^2 - |F_c|^{2)2}$, was minimized, where $w = 1/[(\sigma(F_o))^2 + (0.0269*P)^2 + (6.2058*P)]$ and $P = (|F_o|^2 + 2|F_c|^2)/3$. $R_w(F^2)$ refined to 0.0845, with R(F) equal to 0.0368 and a goodness of fit, S = 1.02. Definitions used for calculating R(F), $R_w(F^2)$ and the goodness of fit, S, are given below.[14] The data were checked for secondary extinction, but no correction was necessary. Neutral atom scattering factors and values used to calculate the linear absorption coefficient are from the International Tables for X-ray Crystallography (1992).[15] All figures were generated using SHELXTL/PC.[16]

Table S5. X-ray structural details for **6** ($C_{27}H_{36}N_2$) Au($C_{23}H_{26}N_2O_3$) – PF_6

CCDC Number	1999230
Empirical formula	C_{50} H_{62} Au F_6 N_4 O_3 P
Formula weight	1108.97

Temperature	100(2) K	
Wavelength	0.71073 Å	
Crystal system	monoclinic	
Space group	P 1 21/n 1	
Unit cell dimensions	a = 17.129(4) Å	α = 90°.
	b = 14.925(3) Å	β = 107.130(5) °.
	c = 19.946(4) Å	γ = 90°.
Volume	4872.8(17) $Å^3$	
Z	4	
Density (calculated)	1.512 Mg/m^3	
Absorption coefficient	3.120 mm^{-1}	
F (000)	2248	
Crystal size	0.36 x 0.3 x 0.09 mm^3	
Theta range for data collection	2.137 to 30.642°.	
Index ranges	-24<=h<=24, -21<=k<=21, -28<=l<=28	
Reflections collected	83413	
Independent reflections	14947 [R(int) = 0.0779]	
Completeness to theta = 25.242°	99.9 %	
Absorption correction	Numerical	
Max. and min. transmission	0.7461 and 0.5510	
Refinement method	Full-matrix least-squares on F^2	
Data / restraints / parameters	14947 / 456 / 656	
Goodness-of-fit on F^2	1.016	
Final R indices [I>2sigma(I)]	R1 = 0.0368, wR2 = 0.0764	
R indices (all data)	R1 = 0.0634, wR2 = 0.0845	
Extinction coefficient	n/a	
Largest diff. peak and hole	2.601 and -2.412 $e.Å^{-3}$	

7. NMR Spectra

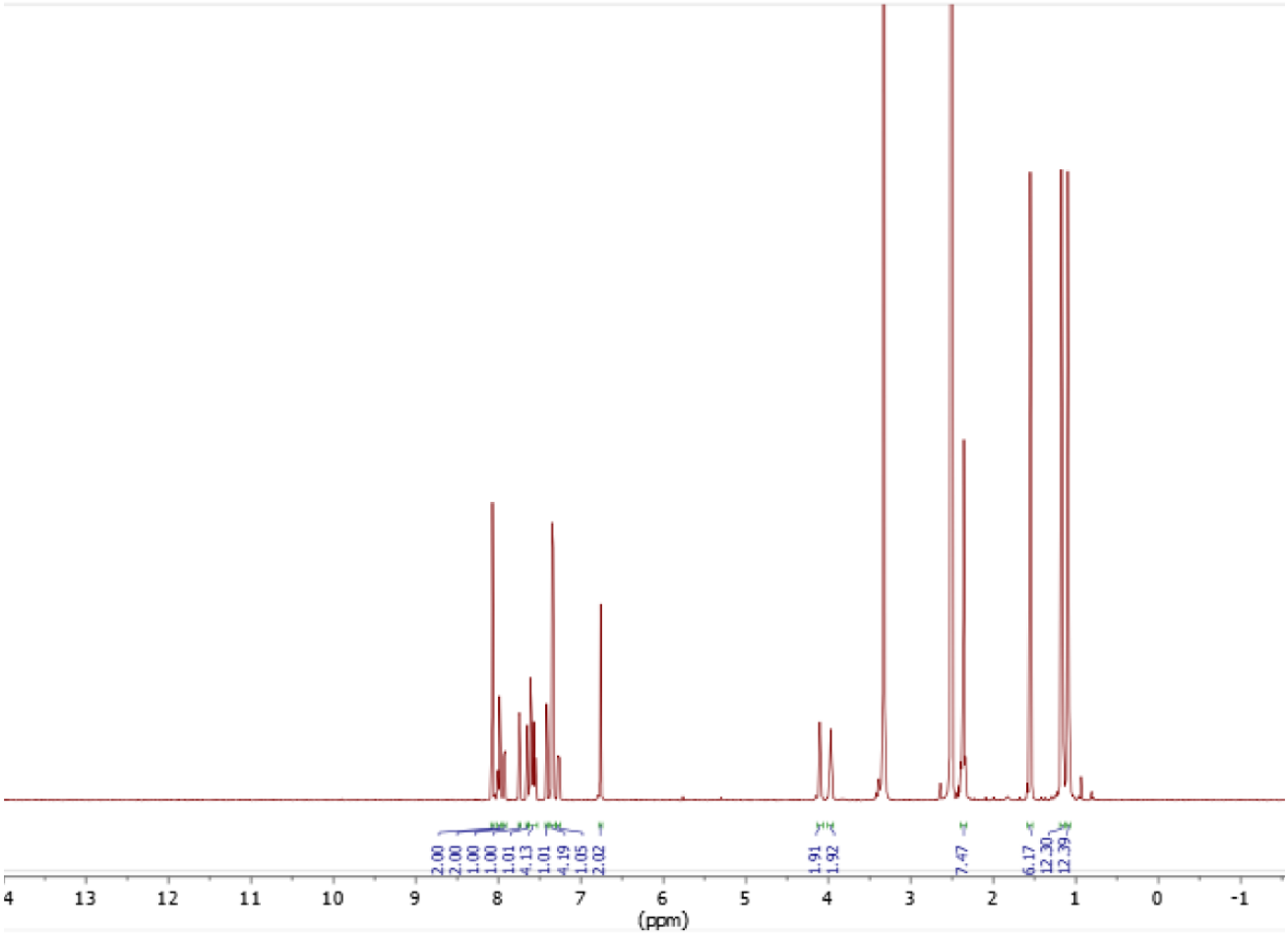

^{1}H NMR spectrum of **4 (500 MHz, 25 °C, DMSO-d_6)**

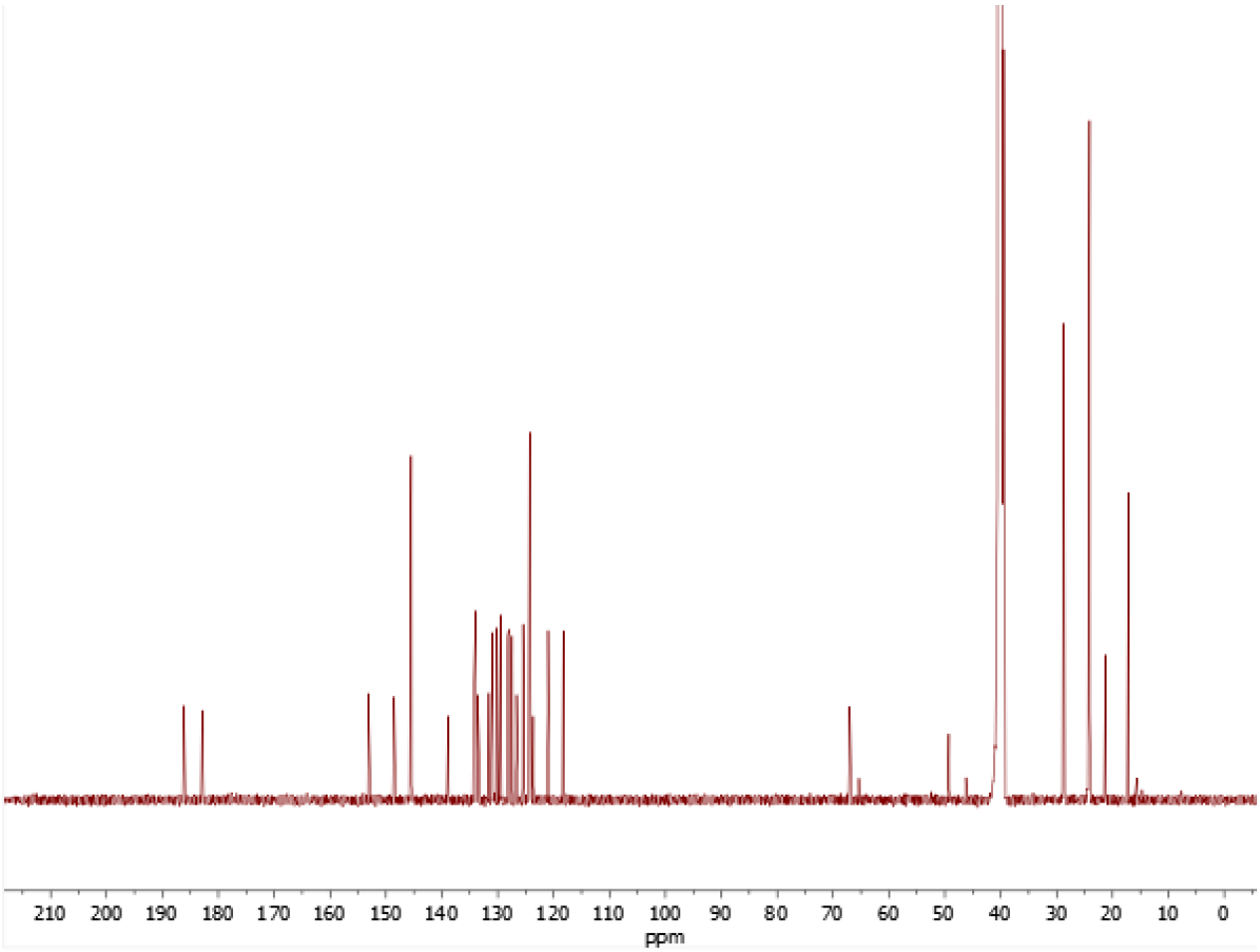

^{13}C NMR spectrum of **4 (126 MHz, 25 °C, DMSO-*d*$_6$)**

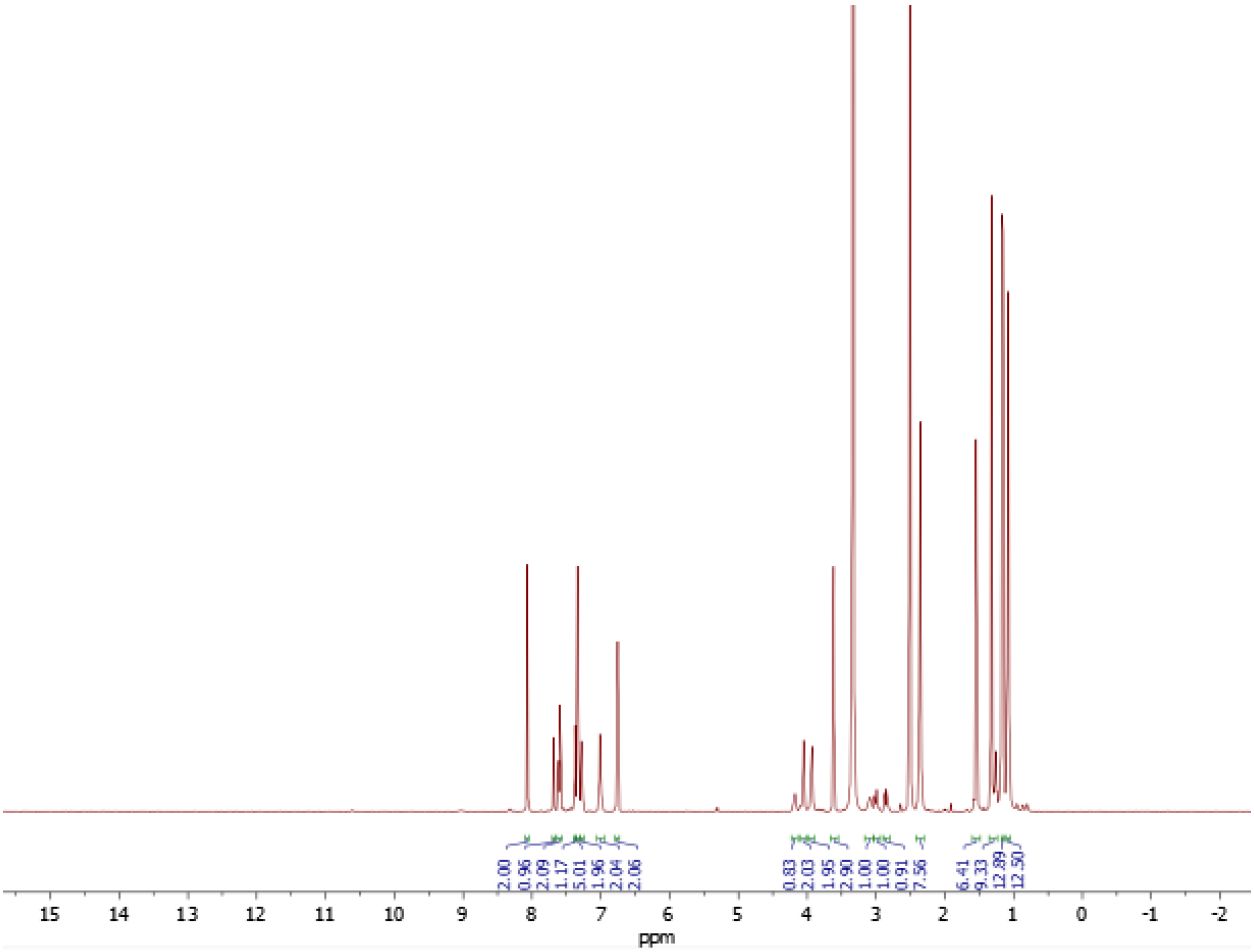

^{1}H NMR spectrum of **8 (500 MHz, 25 °C, DMSO-d_6)**

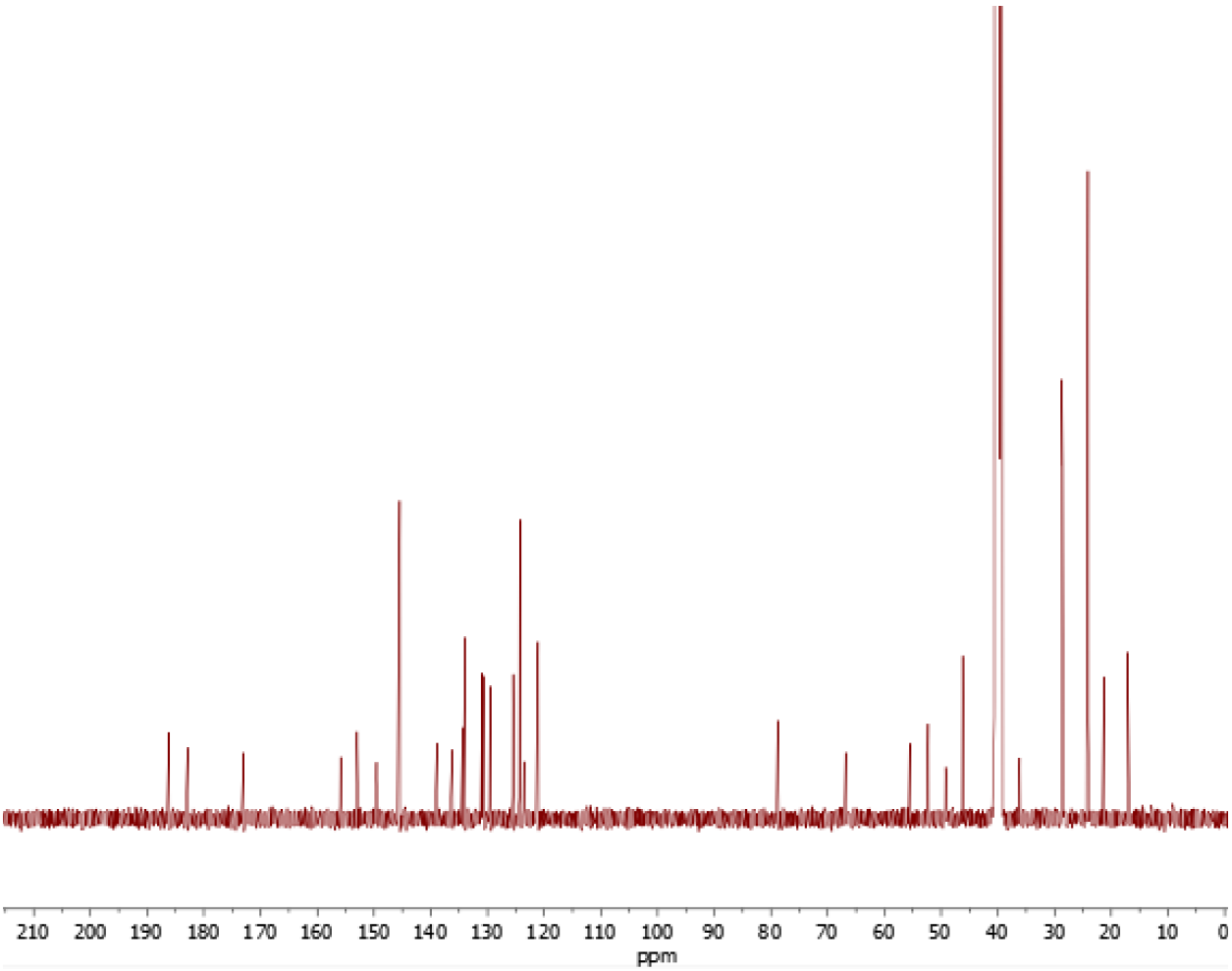

^{13}C NMR spectrum of **8 (126 MHz, 25 °C, DMSO-d_6)**

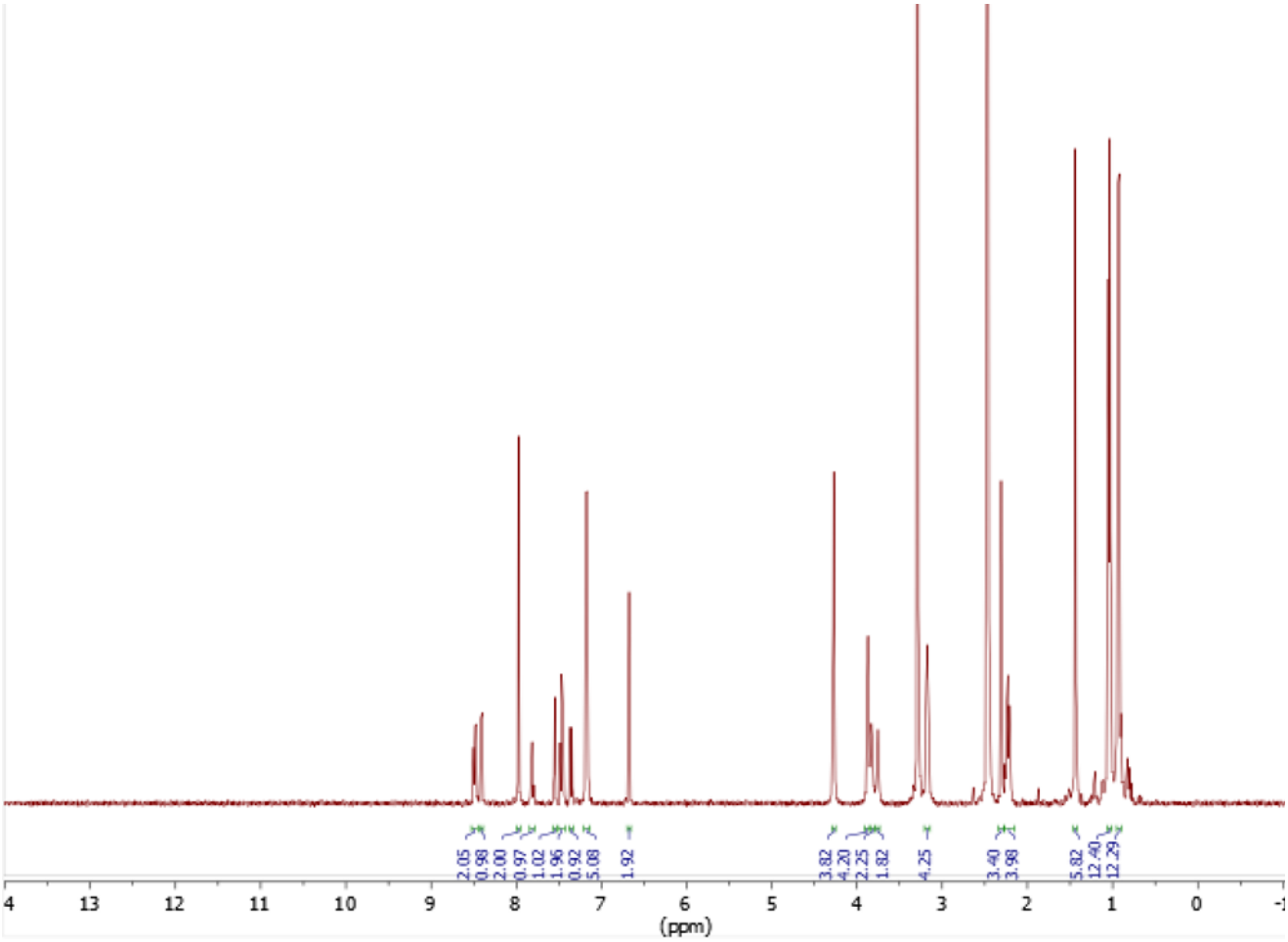

^{1}H NMR spectrum of **5 (500 MHz, 25 °C, DMSO-*d*$_6$)**

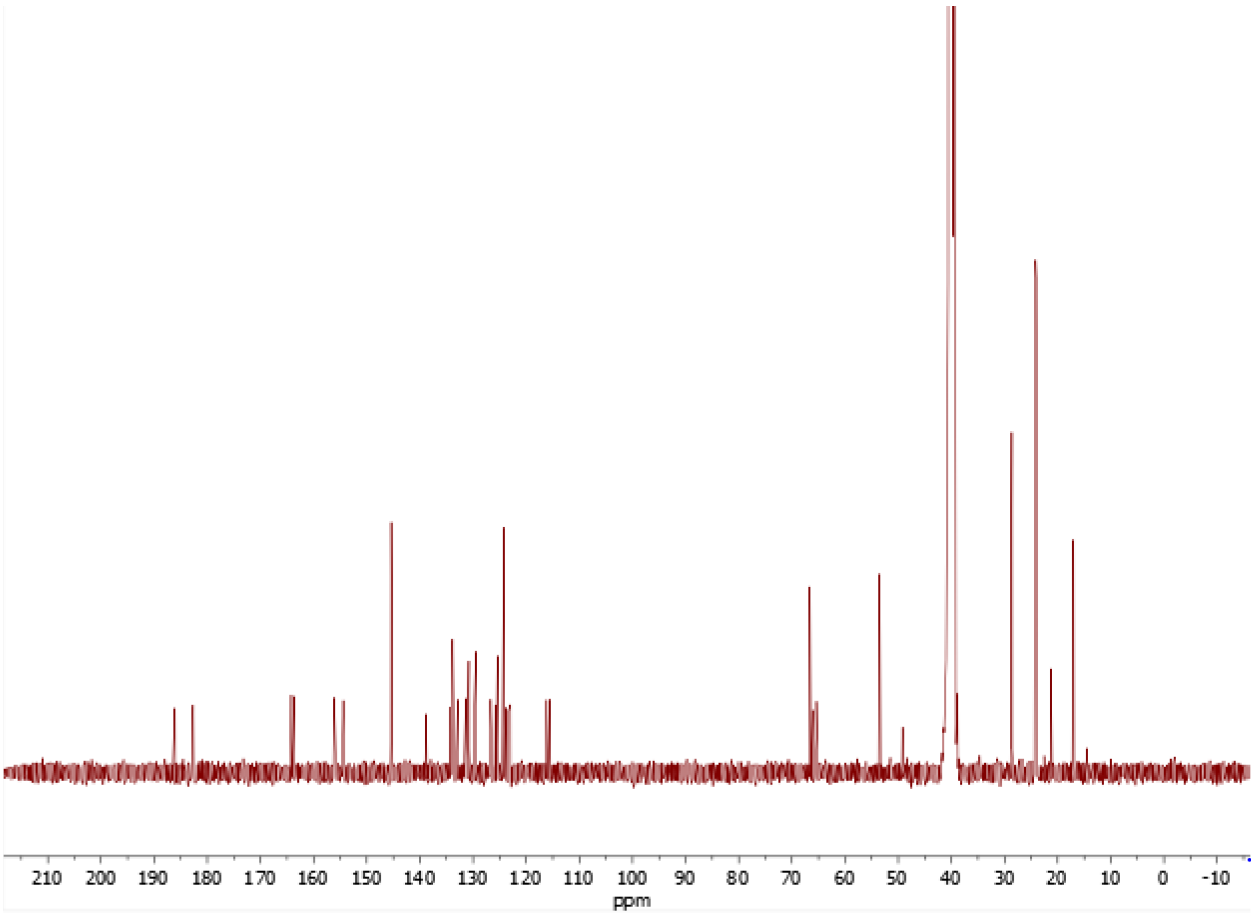

^{13}C NMR spectrum of **5 (126 MHz, 25 °C, DMSO-*d*$_6$)**

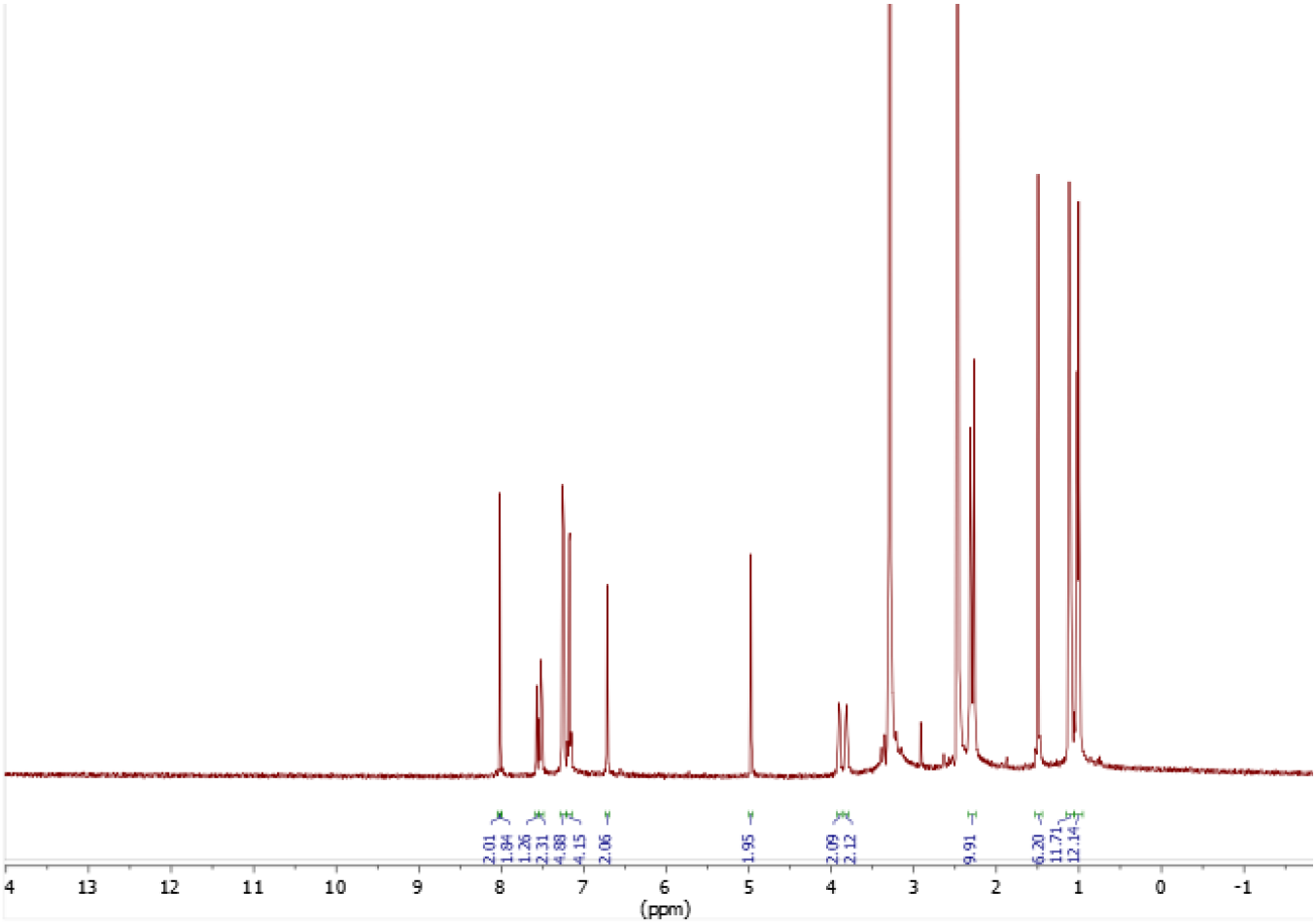

^{1}H NMR spectrum of **6 (500 MHz, 25 °C, DMSO-*d*$_6$)**

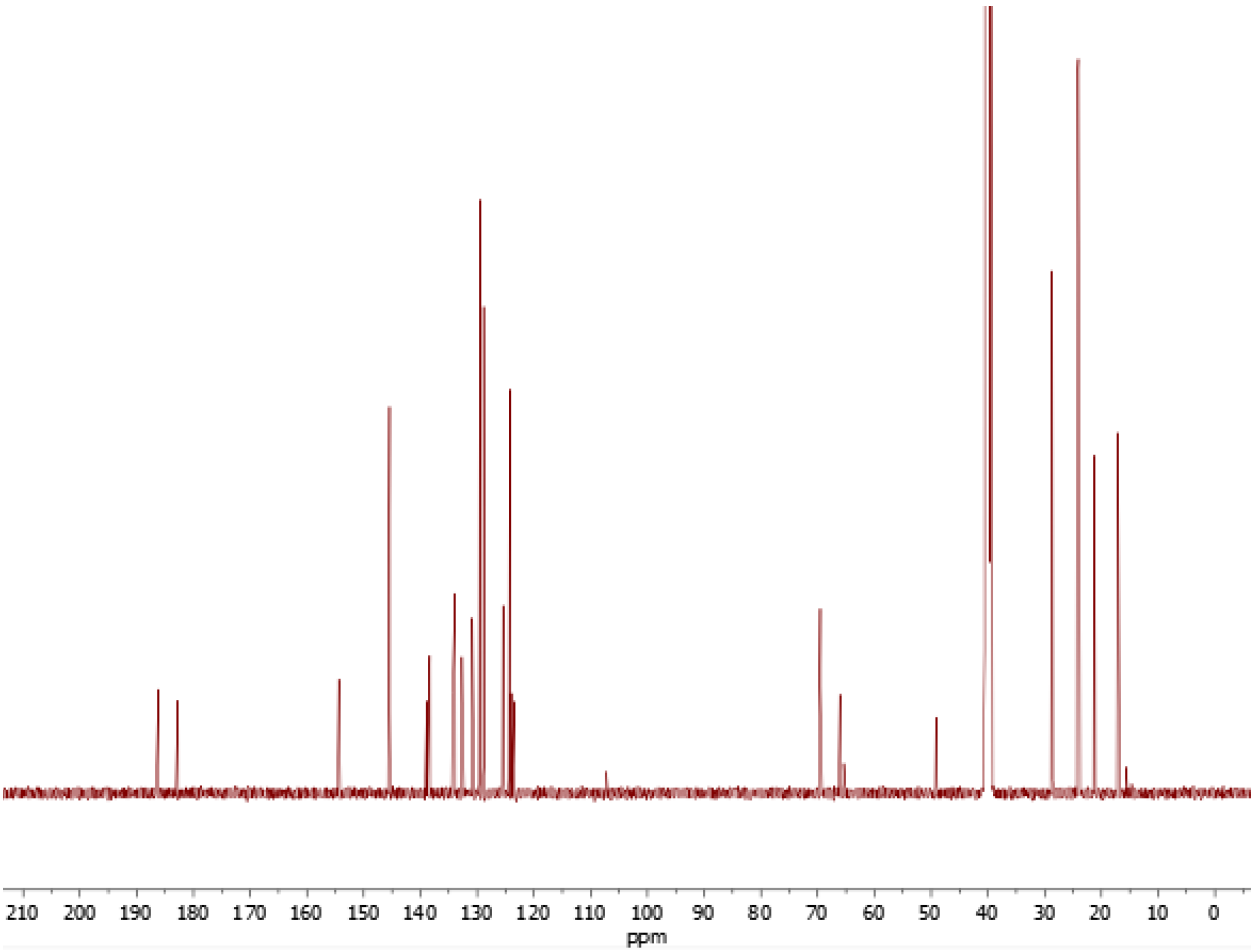

^{13}C NMR spectrum of **6 (126 MHz, 25 °C, DMSO-d_6)**

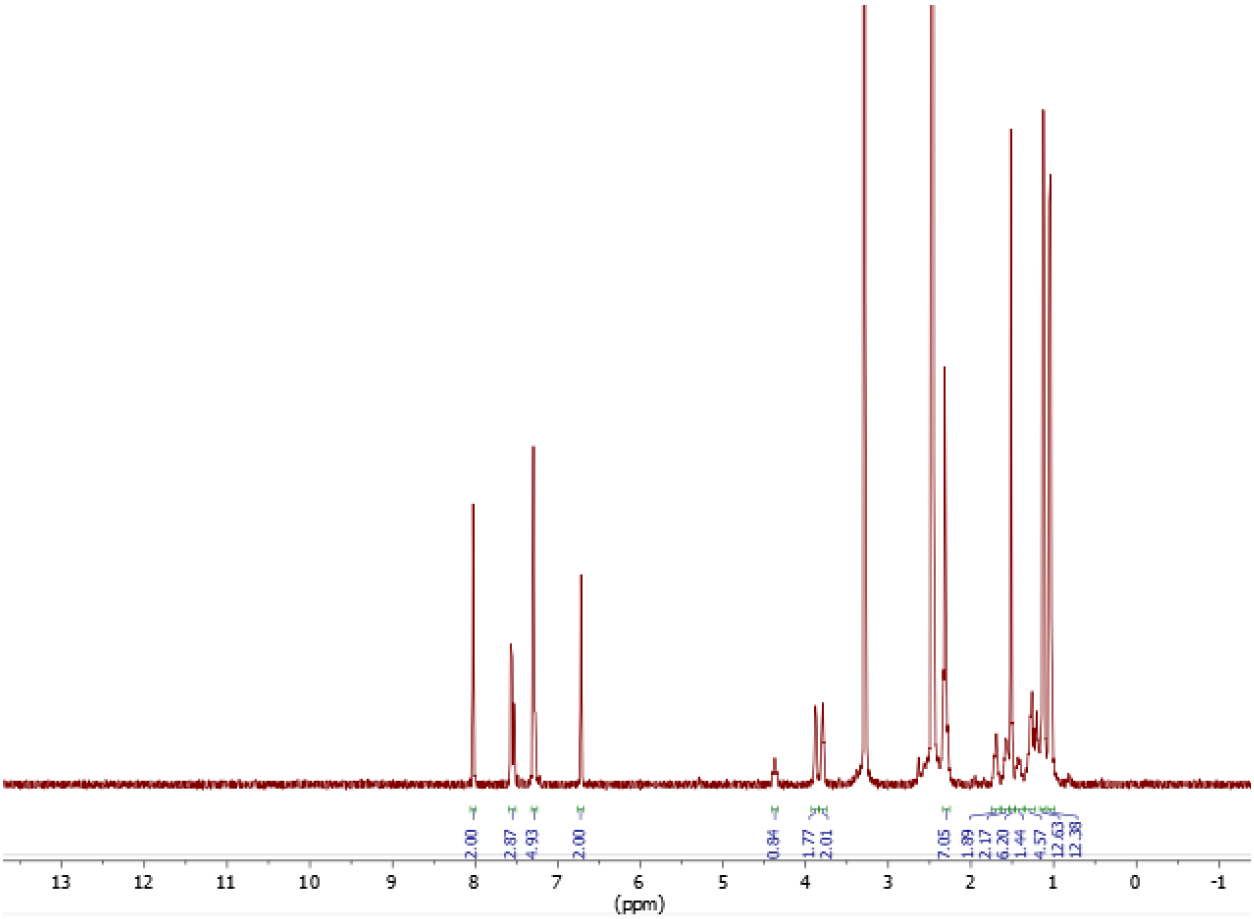

^{1}H NMR spectrum of **7 (500 MHz, 25 °C, DMSO-d_6)**

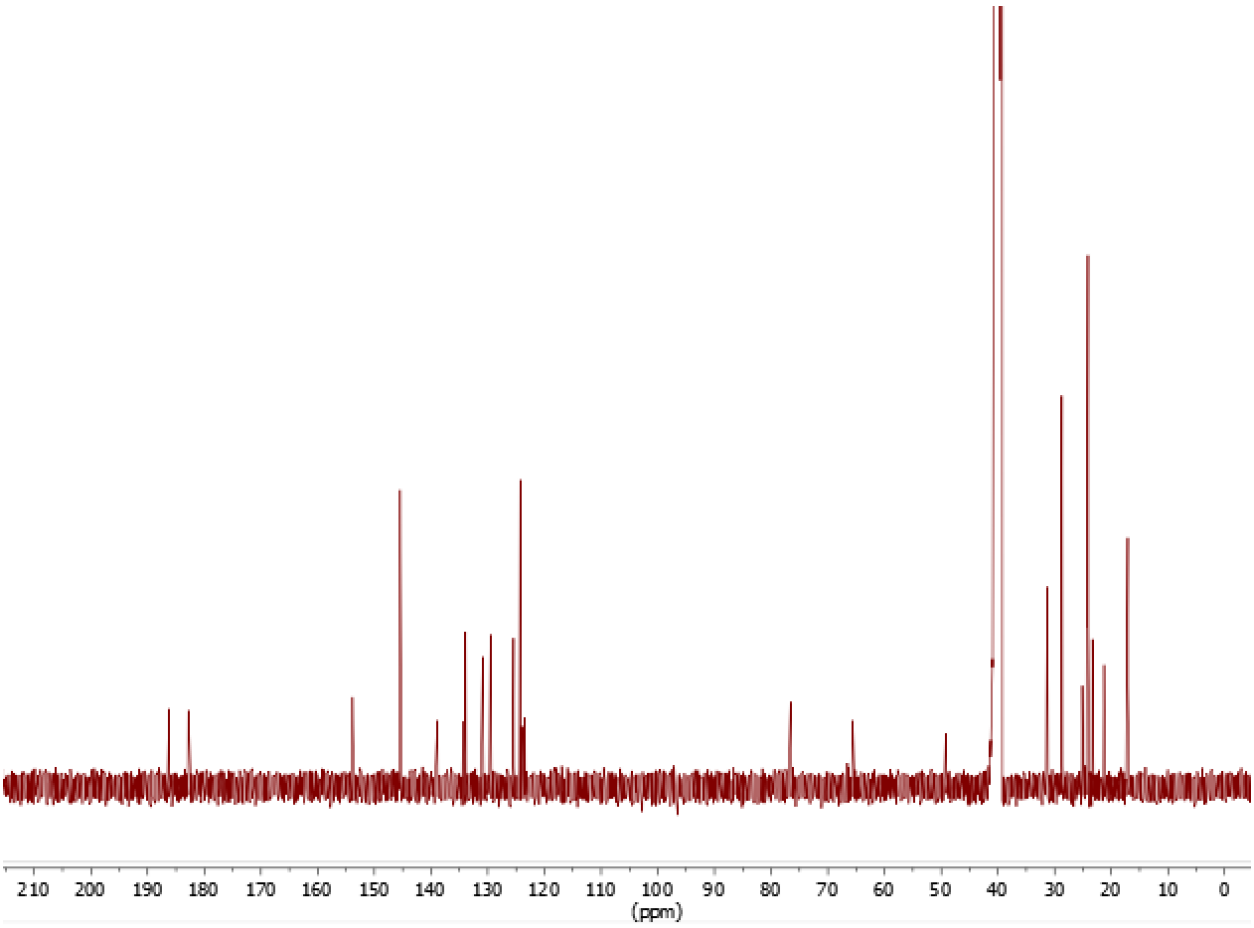

^{13}C NMR spectrum of **7 (126 MHz, 25 °C, DMSO-*d*$_6$)**

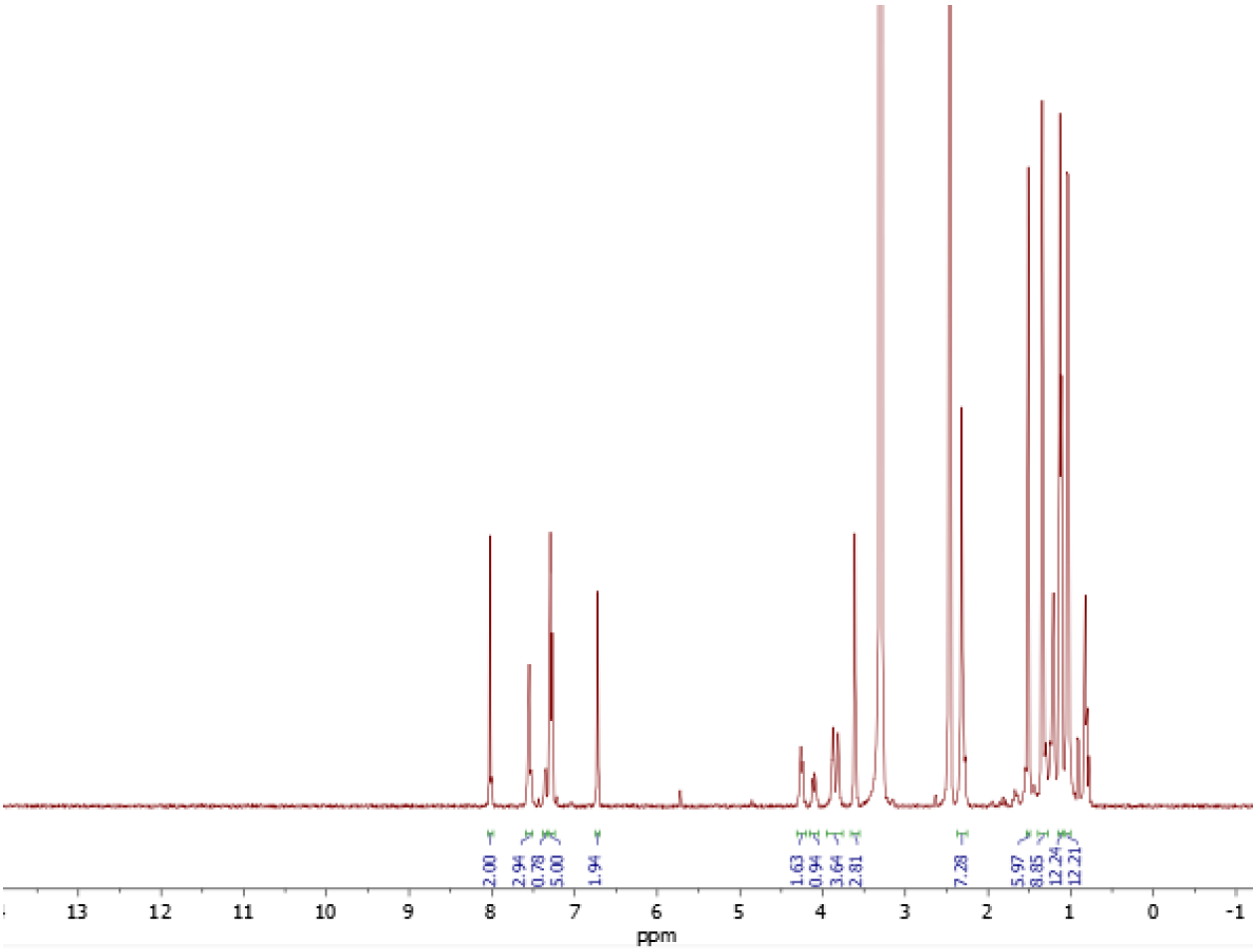

^{1}H NMR spectrum of **9 (500 MHz, 25 °C, DMSO-*d*$_6$)**

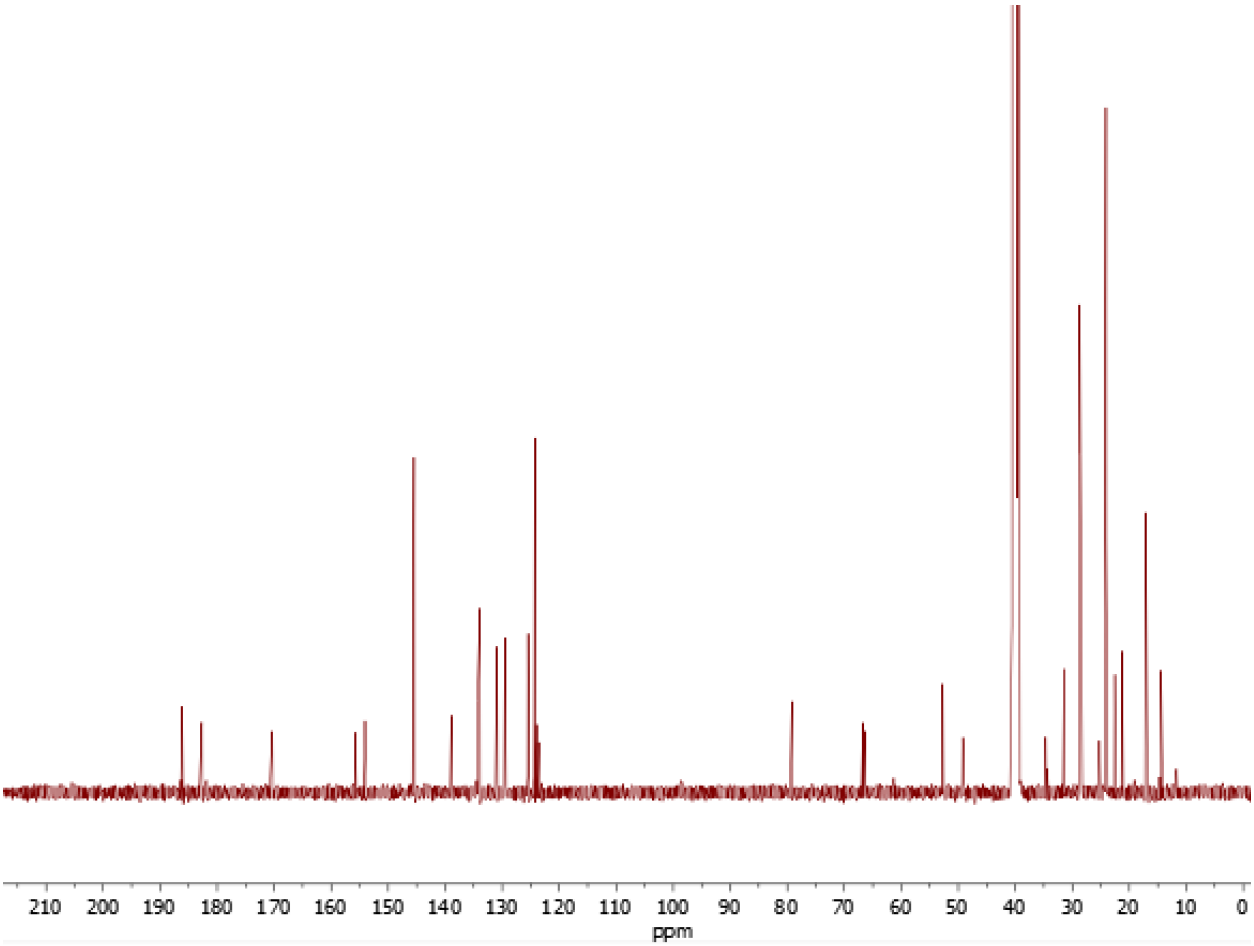

^{13}C NMR spectrum of **9 (126 MHz, 25 °C, DMSO-d_6)**

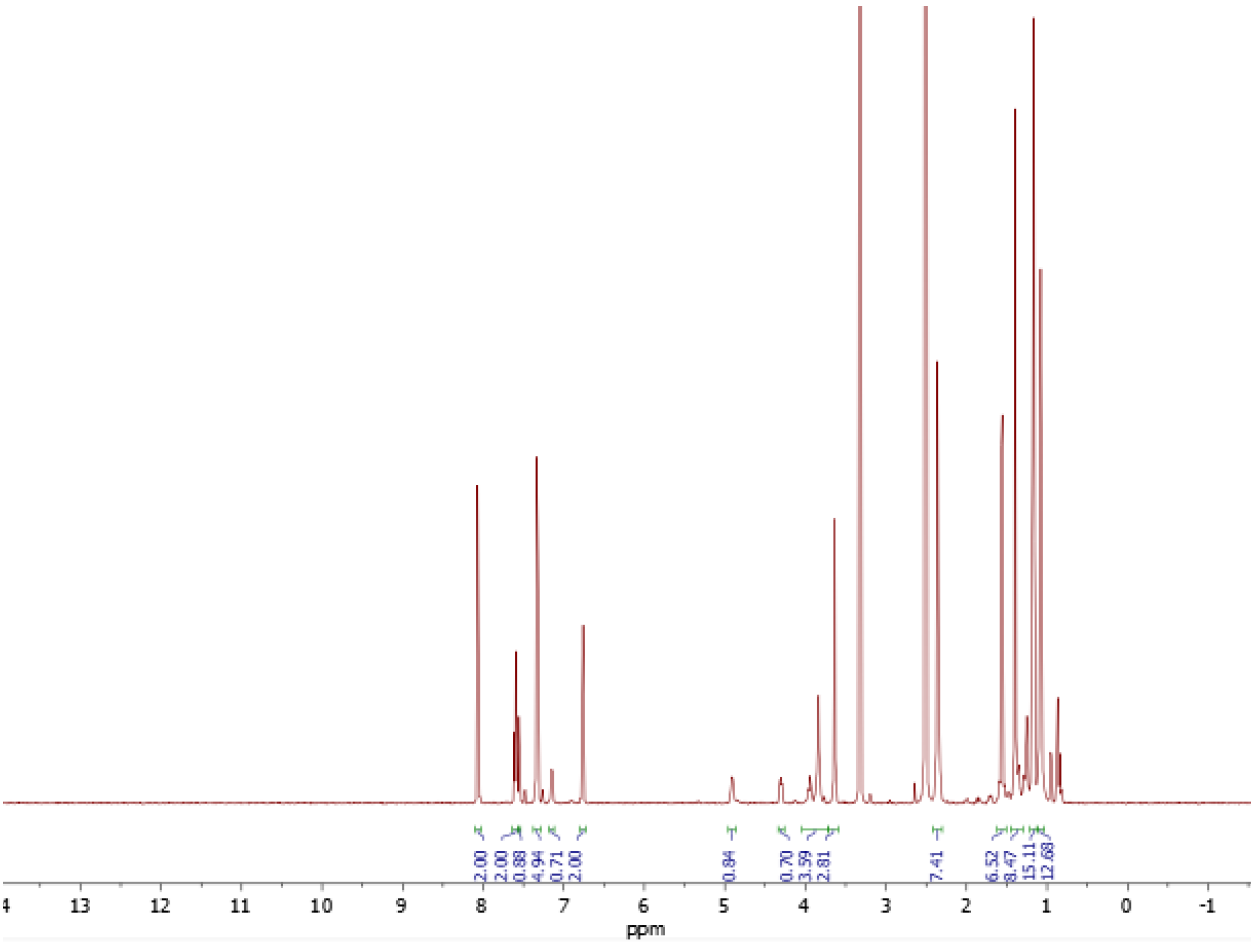

^{1}H NMR spectrum of **10 (500 MHz, 25 °C, DMSO-d_6)**

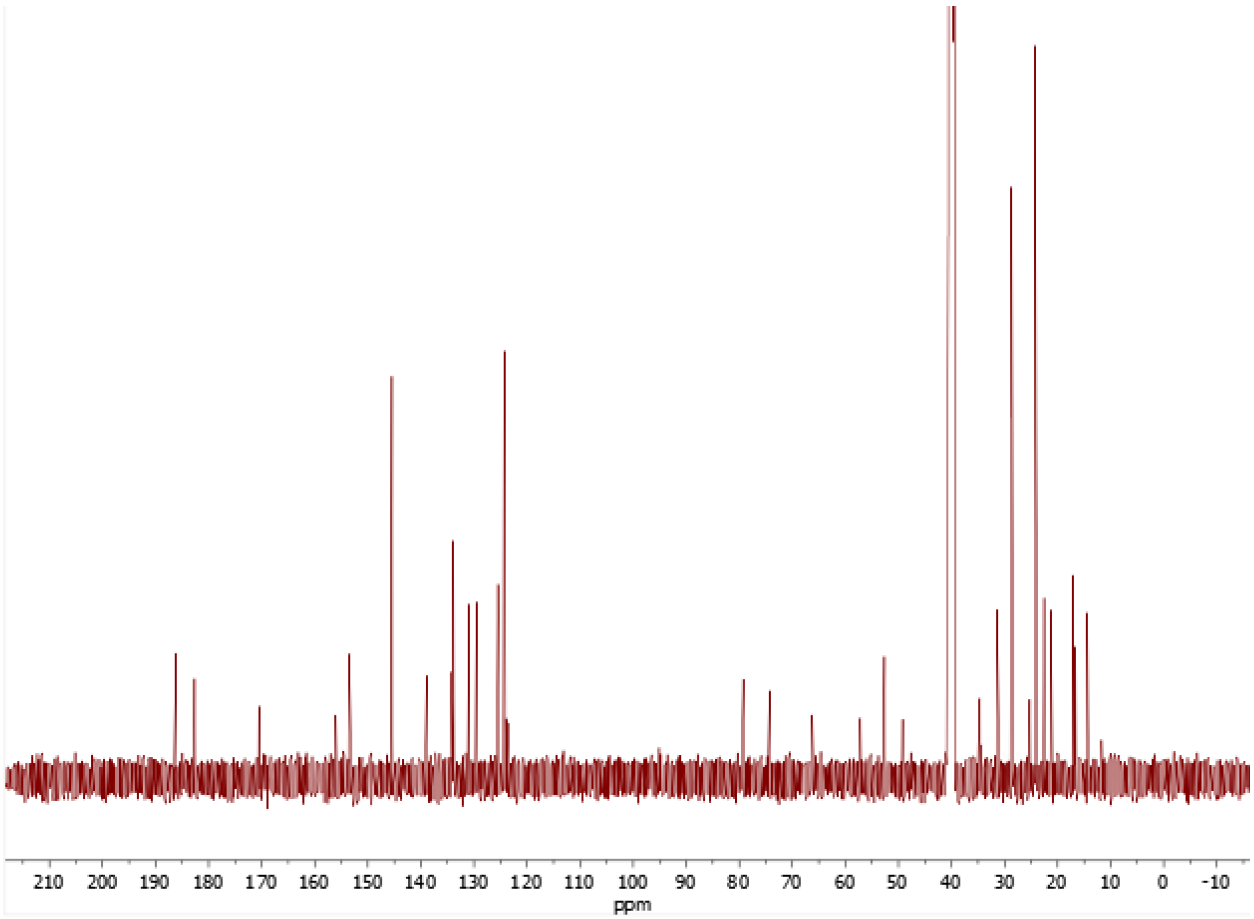

^{13}C NMR spectrum of **10 (126 MHz, 25 °C, DMSO-d_6)**

8. HRMS Spectra:

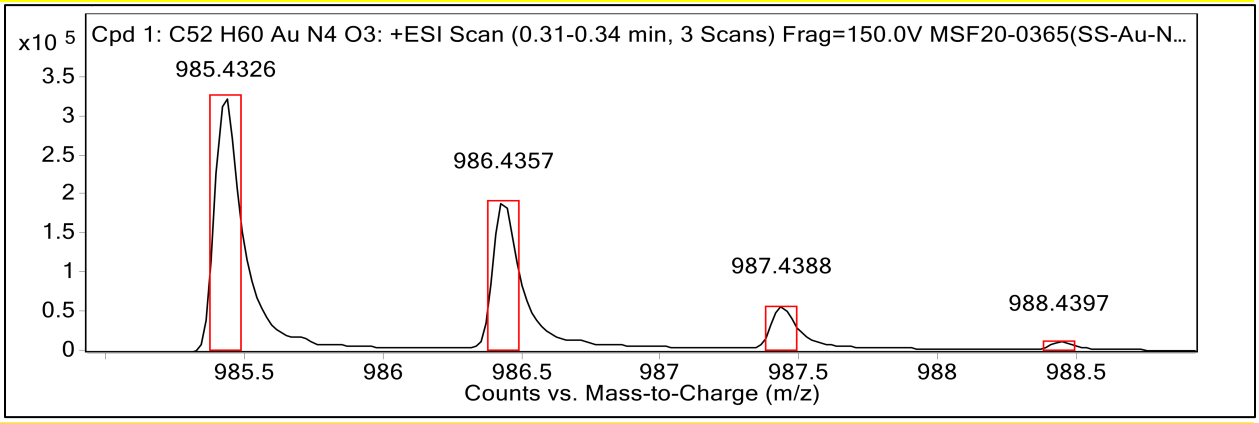

ESI-HRMS (acetonitrile) spectrum of **4**

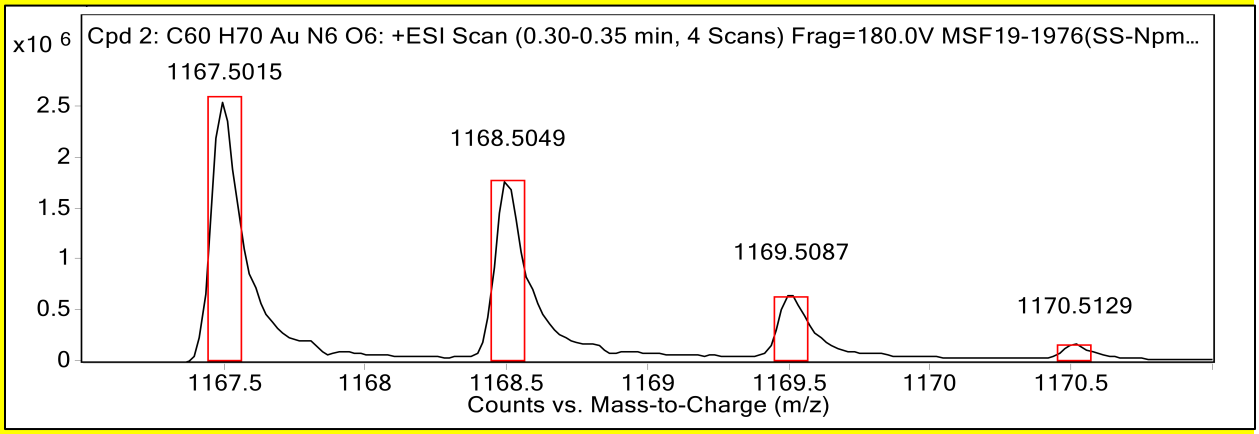

ESI-HRMS (acetonitrile) spectrum of **5**

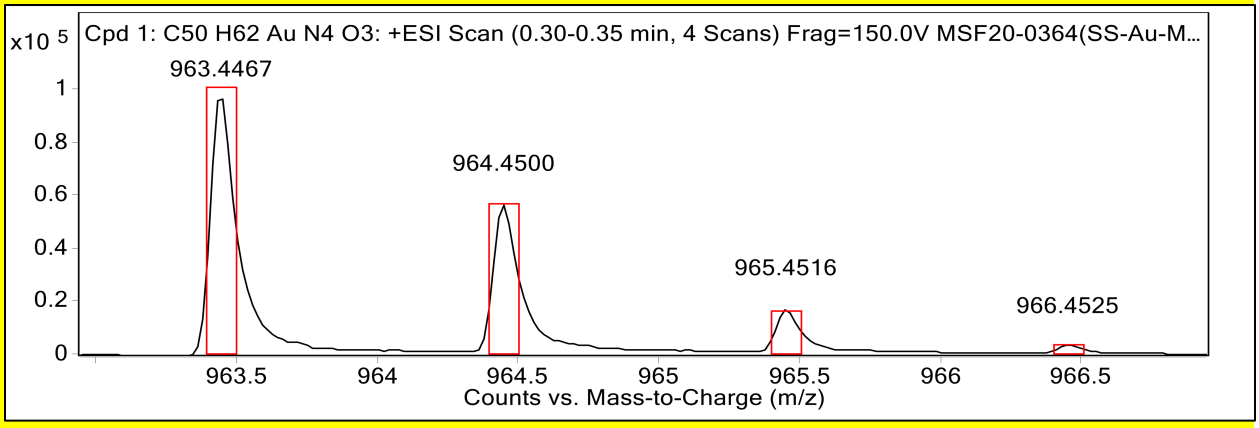

ESI-HRMS (acetonitrile) spectrum of **6**

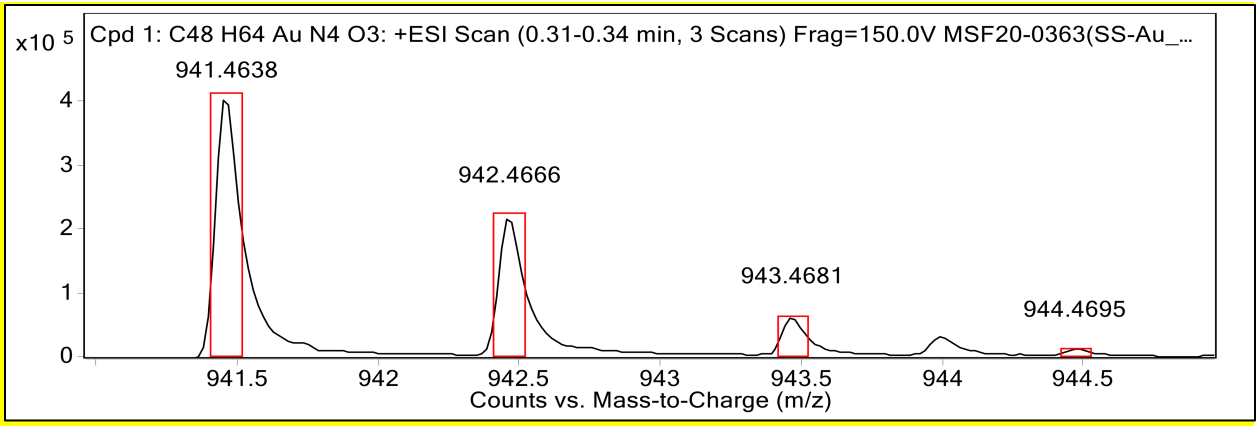

ESI-HRMS (acetonitrile) spectrum of **7**

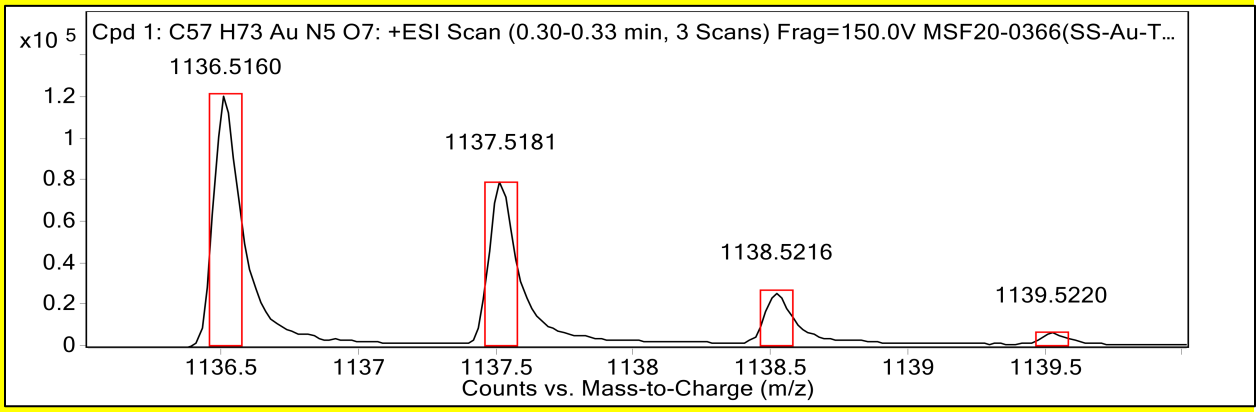

ESI-HRMS (acetonitrile) spectrum of **8**

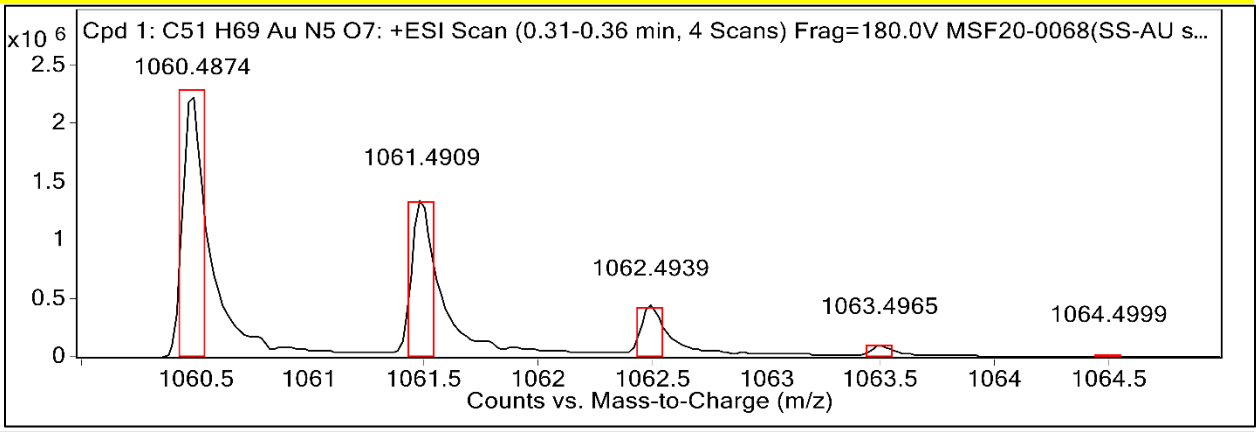

ESI-HRMS (acetonitrile) spectrum of **9**

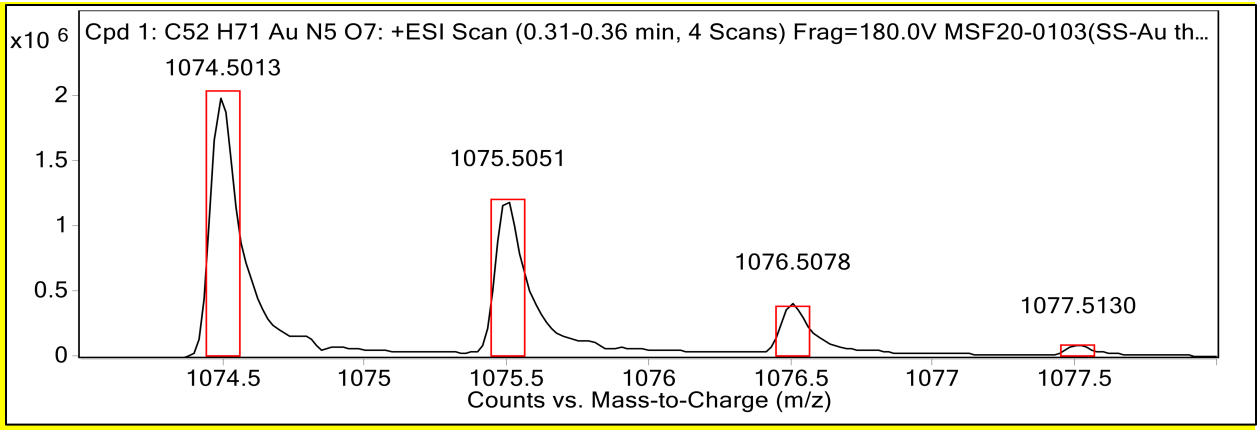

ESI-HRMS (acetonitrile) spectrum of **10**

9. References

1. S. Sen, Y. Li, V. Lynch, K. Arumugam, J. L. Sessler and J. F. Arambula, *Chem. Commun.*, 2019, **55**, 10627–10630.
2. A. Ishizaki, T. R. Calhoun, G. S. Schlau-Cohen and G. R. Fleming, *Phys. Chem. Chem. Phys.*, 2010, **12**, 7319–7337.
3. A. M. Krause-Heuer, W. S. Price and J. R. Aldrich-Wright, *J. Chem. Biol.*, 2012, **5**, 105–113.
4. S. Nusrat, M. K. Siddiqi, M. Zaman, N. Zaidi, M. R. Ajmal, P. Alam, A. Qadeer, A. S. Abdelhameed and R. H. Khan, *PLoS One*, 2016, **11**, 1–20.
5. J. R. Lakowicz, Fluorophores. Principles of fluorescence spectroscopy: Springer, 1999, pp. 63–93.
6. Z.-Y. Tian, L.-N. Song, Y. Zhao, F.-L. Zang, Z.-H. Zhao, N.-H. Chen, X.-J. Xu and C.-J. Wang, *Molecules*, 2015, **20**, 16491–16523.
7. J. Liu, Y. He, D. Liu, Y. He, Z. Tang, H. Lou, Y. Huo and X. Cao, *RSC Adv.*, 2018, **8**, 7280–7286.
8. CrysAlisPro. Rigaku Oxford Diffraction (2019). CrysAlisPro Software System, 1.171.40.53.
9. G. M. Sheldrick, *Acta Cryst. A*, 2015, **71**, 3-8.
10. G. M. Sheldrick, *Acta Cryst. C*, 2015, **71**, 9-18.
11. A. L. Spek, *Acta Cryst. D*, 2009, **65**, 148-155.
12. O. V. Dolomanov, L. J. Bourhis, R. J. Gildea, J. A. K. Howard, and H. Puschmann, *J. Appl. Cryst.*, 2009, **42**, 339-341.
13. L. J. J. Farrugia, *Appl. Cryst.*, 1999, **32**, 837-838.
14. $R_w(F^2) = \{\Sigma w(|F_o|^2 - |F_c|^2)^2/\Sigma w(|F_o|)^4\}^{1/2}$ where w is the weight given each reflection.
    $R(F) = \Sigma(|F_o| - |F_c|)/\Sigma|F_o|\}$ for reflections with $F_o > 4(\sigma(F_o))$.
    $S = [\Sigma w(|F_o|^2 - |F_c|^2)^2/(n - p)]^{1/2}$, where n is the number of reflections and p is the number of refined parameters.
15. A. J. C. Wilson, *International Tables for X-ray Crystallography Vol. C*. Boston: Kluwer Academic Press, 1992, Tables 4.2.6.8 and 6.1.1.4.
16. Sheldrick, G. M. (1994). *SHELXTL/PC (Version 5.03)*. Siemens Analytical X-ray Instruments, Inc., Madison, Wisconsin, USA.
17. SAINT V8.34A Bruker AXS Inc, (2013), Madison, WI.